

Physico-chemical foundations of particle-laden fluid interfaces^{*}

Armando Maestro¹, Eva Santini², and Eduardo Guzmán^{3,4,a}

¹ Institut Laue-Langevin, 71 avenue des Martyrs, CS 20156, 38042 Grenoble, Cedex 9, France

² Istituto di Chimica della Materia Condensata e di Tecnologia per l'Energia (ICMATE), U.O.S. Genova-Consiglio Nazionale delle Ricerche (CNR), Via De Marini 6, 16149 Genova, Italy

³ Departamento de Química Física I, Universidad Complutense de Madrid, Ciudad Universitaria s/n, 28040 Madrid, Spain

⁴ Instituto Pluridisciplinar, Universidad Complutense de Madrid, Paseo Juan XXIII, 1, 28040 Madrid, Spain

Received 31 March 2018 and Received in final form 2 July 2018

Published online: 28 August 2018

© EDP Sciences / Società Italiana di Fisica / Springer-Verlag GmbH Germany, part of Springer Nature, 2018

Abstract. Particle-laden interfaces are ubiquitous nowadays. The understanding of their properties and structure is essential for solving different problems of technological and industrial relevance; *e.g.* stabilization of foams, emulsions and thin films. These rely on the response of the interface to mechanical perturbations. The complex mechanical response appearing in particle-laden interfaces requires deepening on the understanding of physico-chemical mechanisms underlying the assembly of particles at interface which plays a central role in the distribution of particles at the interface, and in the complex interfacial dynamics appearing in these systems. Therefore, the study of particle-laden interfaces deserves attention to provide a comprehensive explanation on the complex relaxation mechanisms involved in the stabilization of fluid interfaces.

1 Introduction

The ubiquity of particle-laden interfaces in both nature and industry has driven, in the last thirty years, the development of an important research field, which tries to unravel the physico-chemical bases underlying the attachment of particles to interfaces, especially fluid ones, *i.e.* liquid/vapor and liquid/liquid interfaces [1–8]. The extensive research focused on the understanding of such systems has raised many questions, associated with the relationship existing between the interactions occurring at the fluid interface (particle-particle, particle-fluids and fluid-fluid interactions), and the structure and properties of the particle-laden interface [2, 6, 9–14]. The comprehensive understanding of the aforementioned aspects is mandatory for developing processes and products for technological purposes based on the interactions of particles with interface [5, 8, 14–18]. This is a challenge, involving both practical and theoretical efforts, aimed to develop a framework providing a description of complex interplay existing between different physico-chemical properties, *e.g.* particle wettability, size, shape, surface charge, and chemical na-

ture of the particles and the interface, with the relative dielectric constant of the phases playing a main role on the trapping of the particles at fluid interfaces and the interactions [12].

Among the fields in which particle-laden interfaces play a key role are included: stabilization of dispersed systems (foams, emulsions, or thin films), flotation processes, encapsulation, pharmaceutical formulations, food technology and catalysis [2, 15, 19–24]. However, the important development of such field has also raised different questions related to the toxicity for human and environmental health of particles, especially those in the nanosize scale [25–29]. Thus, further developments on this field deserve a detailed analysis of both the physico-chemical bases underlying the fabrication processes and the potential risks associated with such processes and materials [30].

The assembly of particles at fluid interfaces leads to a broad range of structures, among which is possible to find crystalline 2D layers or fractal patterns of particle aggregates [9, 10, 31–34]. It is expected that this variety of structures affects the mechanical performance of interfaces [6, 35], *e.g.* governing the collapse mechanism of the interface through the appearance of buckling, jamming, or squeezing-out phenomena upon compression or densification of the layer [3, 36, 37]. This has been exploited in several applications which rely on the response of particle-laden interfaces upon dilation and/or shear de-

^{*} Contribution to the Topical Issue “Flowing Matter, Problems and Applications”, edited by Federico Toschi, Ignacio Pagonabarraga Mora, Nuno Araujo, Marcello Sega.

^a e-mail: eduardogs@quim.ucm.es

formations [7, 8, 38–41]. Furthermore, the understanding of the interfacial relaxation processes of particle layers against an external mechanical perturbation plays a central role for the stabilization of foams and emulsions. In such systems, the coating of bubbles or drops by particle layers provides mechanical stability to the interface, preventing destabilization phenomena, such as coalescence and Ostwald ripening, thus hindering the drainage by a gravitational field. This has been exploited from the seminal works by Ramsden [42] and Pickering [43] more than one century ago. Therefore, deepening on the physico-chemical aspects underlying the performance of particle-laden interfaces under dynamic conditions will result in an improvement of their application in the fabrication of consumer products [44].

Particle-laden interface can be prepared following two different approaches [1, 45]. The former one considers the direct self-assembly at the interface of particles from bulk dispersions leading to the formation of the so-called adsorbed monolayers [46, 47]. Whereas, the latter is based on the direct spreading at the fluid interface of a controlled volume of a particle dispersion, leading to the formation of a spread monolayer [9, 10]. The interfacial density of particles is controlled in the latter case by the spread amount, while for the adsorbed monolayers it depends strongly on the particle affinity for the fluid interface.

This review is focused on providing a comprehensive understanding on the fundamental bases underlying the relaxation mechanisms involved in the equilibration of particle-laden interfaces. For this purpose, we will start describing, firstly, the main physico-chemical aspects governing the attachment of particles to fluid interfaces, and, subsequently their response when they undergo mechanical deformations. The last part of this review will provide a briefly discussion on the application of particle-laden interfaces on the stabilization of dispersed systems.

It is worth mentioning that particles at fluid interfaces behave in many aspects as surfactants [2, 48]. Thus, the use of particles for replacing surfactants in technological applications (foams and emulsions stabilization), has undergone a spectacular development in recent years. However, the different length scales involved in particles and surfactants, and the different nature of the attachment of particles and surfactant at the fluid interface leads to important differences in the physico-chemical behavior of particles and surfactants at interfaces.

2 Contact angle: controlling the particle attachment at interfaces

Despite the most fundamental bases governing the adsorption of particles at fluid interfaces have been studied extensively in the last thirty years, several aspects still remain unclear and deserve further studies [1–3, 6, 12–14, 44]. This is mainly due to the multiphase character of particle-laden interfaces which makes necessary to take into account the role of three interfaces: two fluid/solid and one fluid/fluid (see fig. 1 for a schematic representation).

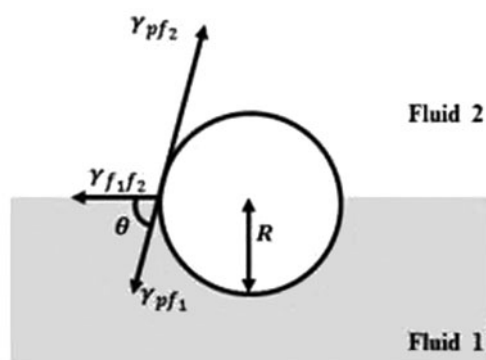


Fig. 1. Sketch representing the typical situation of a particle attached to an arbitrary fluid interface in which θ represents the contact angle or relative wettability of the particle by the interface, R is the particle radius, and $\gamma_{f_1 f_2}$, $\gamma_{p f_1}$ and $\gamma_{p f_2}$ are the interfacial tensions corresponding to the fluid/fluid interface and the two fluid/solid (fluid/particle) interfaces, respectively.

The accumulation of particles at fluid interfaces results from the complex balance between different types of interactions, with the electrostatic and capillary interactions playing a central role [1, 12, 34]. The result of such balance drives the particles until their equilibrium position in relation to the separation plane between the two phases defined by the interface, and allows one to define the relative wettability of solid particles by the two fluid phases, *i.e.* the three phase contact angle θ or simply contact angle (see fig. 1).

The contact angle plays a role for the adsorption of particles at fluid interface similar to that of the HLB (hydrophilic-lipophilic balance) in molecular species, defining the preferential partition of particles between both phases [48, 49], which is related to an asymmetric distribution of the interactions through the two fluid phases [50, 51]. This leads to two limits cases, when the fluid phases present very different nature: $\theta = 0\text{--}10^\circ$ and $\theta = 170\text{--}180^\circ$. In those cases, the adsorption at the fluid phase is hindered and particles remain preferentially in the hydrophilic and in the hydrophobic phases, respectively. Therefore, it is possible to assume that partial wetting of particles for both fluid phases is a key factor on their adsorption at the fluid interface. Figure 2 shows a schematic representation of the preferential distribution of particles between the fluid phases as the contact angle changes.

The position of the particle in relation to the interfacial plane allows defining its hydrophilicity-hydrophobicity. When water/oil interfaces are considered, it is frequently to define particles as hydrophilic for angles $\theta < 90^\circ$, becoming hydrophobic when $\theta > 90^\circ$. It is worth mentioning that the preferential distribution of particles between the fluid phases plays an important role in the control of the relaxation mechanisms of particle-laden interfaces and consequently in their technological applications [52, 53].

The contact angle θ can be defined assuming the existence of a mechanical equilibrium between the different forces operating at the particle-laden interface. This con-

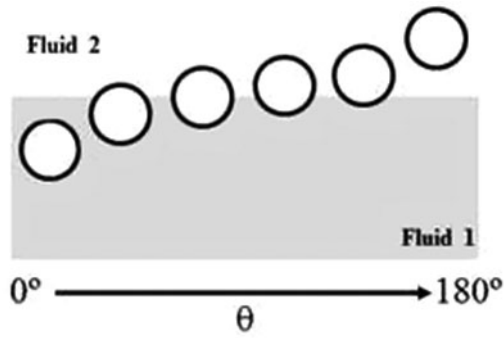


Fig. 2. Idealized representation of the relative position of an arbitrary particle in relation to the interfacial plane defined by the fluid interface as function of its contact angle.

dition is given by Young's equation [54, 55]

$$0 = \gamma_{pf_2} - \gamma_{pf_1} - \gamma_{f_1f_2} \cos \theta, \quad (1)$$

which can be reordered as follows:

$$\cos \theta = \frac{\gamma_{pf_2} - \gamma_{pf_1}}{\gamma_{f_1f_2}}. \quad (2)$$

Despite the role of the contact angle has been neglected in studies on particle-laden interfaces, from its definition it is evident its importance for controlling the balance of energies at the interface. Thus, a reliable determination of the contact angle of particles attached at fluid interfaces is a key for deepening on the complex phenomenology occurring in this type of systems. This has stimulated the interest for developing methodologies allowing for the determination of this important parameter [4, 46, 47, 56–67]. It is worth mentioning that the above definition of the contact angle neglects the roles of the particle roughness and of the line tension, which affect significantly the adsorption at fluid interfaces of nanosized particles [68, 69]. In particular, the line tension modifies the energetic landscape associated with the attachment of particles at the interface. However, the role of the line tension decreases fast with the increase of the particle size and, for most practical cases, the attachment of particles at fluid interface can be described without considering the role of the line tension. For these reasons, no further discussion about its role will be included in this review. Further details on the effect of the line tension in the attachment of particles to fluid interfaces can be found in refs. [67, 70, 71].

The attachment of particles to fluid interfaces is defined by the difference between the energies of a particle in the bulk suspension and at the interface. For small spherical particles, in which gravity effects can be neglected, the attachment energy, μ_w , is given by the following expression:

$$\mu_w = -\pi R^2 \gamma_{f_1f_2} (1 \pm \cos \theta)^2, \quad (3)$$

where R is referred to the radius of the particle and the \pm sign indicates the position of the particles in relation to the interfacial plane. Therefore, (+) is used for hydrophobic particles that are centered above the interfacial plane, and (–) indicates the hydrophilicity of the particles which

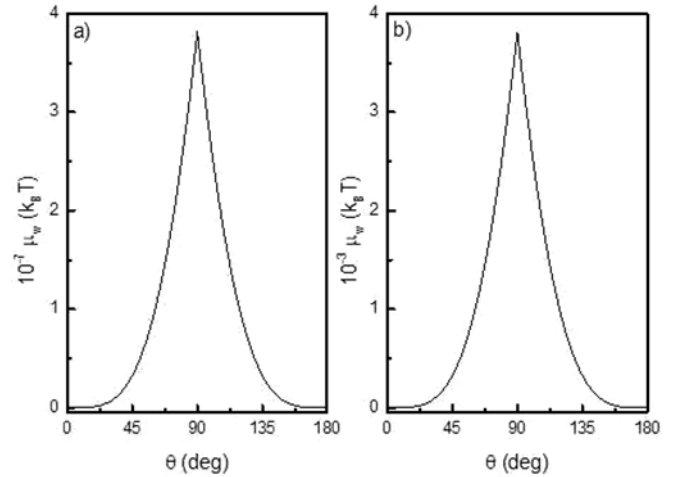


Fig. 3. Dependence of the attachment energy on the contact angle for the adsorption of colloidal particles with different sizes, $R = 1 \mu\text{m}$ (a) and $R = 10 \text{nm}$ (b), at an arbitrary fluid/fluid interface ($\gamma_{f_1f_2} = 50 \text{mN/m}$). Note the differences in the values of the energy scale.

appears centered below the interfacial plane. Figure 3 represents the attachment energies at an arbitrary fluid/fluid interface corresponding to colloidal particles with two different sizes.

Particles at fluid interfaces present an attachment energy that overcomes in most cases several times the thermal energy $k_B T$, with k_B being the Boltzmann constant and T the absolute temperature [34]. The analysis of eq. (3) evidences clearly that the reversibility or irreversibility of the particle attachment depends on the size, R , chemical nature of the particles, θ , and on the nature of the interface, $\gamma_{f_1f_2}$. In general, microparticles are trapped at fluid/fluid interfaces with energies 10^6 – 10^7 times $k_B T$ which almost ensure the irreversibility of their attachment. However, the situation is more complex when nanoparticles are considered, and the irreversibility of their adsorption is strongly dependent on particles size, appearing for the smallest particles adsorption-desorption equilibria similar to those found for conventional surfactants [72]. Wi *et al.* [73] pointed out that the attachment at fluid interfaces of particles with diameter above 10 nm can be considered irreversible. It is worth mentioning that the reversibility or irreversibility of the adsorption of particles at fluid interfaces represents a key role on the control of the particle interactions within the interface and consequently determines the equilibrium structure of the particle assembly [74]. The existence of an irreversible attachment does not mean that particles remain constrained at fixed position in a quasi-2D layer. They are free to diffuse along the 2D plane defined by the interface. In addition, particles at fluid interfaces are undergone to continuous fluctuations around their equilibrium positions due to thermal and/or capillary deformation of the interface.

The above discussion evidences the importance of particles wettability on their adsorption at fluid interfaces. Particles wettability can be tuned through any methodology enabling for their surface modification [3], involving

also changes on the chemical or physical nature of the particles. The chemical modification is generally based on the irreversible attachment of ligands to the particles surface through a chemical reaction that leads to the formation of covalent bonds, *e.g.* thiol onto gold surfaces or silanization reactions of SiO₂ [75–77]. The modification of particles wettability using physical procedures involves the interaction between particles and chemical species, generally surfactants (molecular or polymeric ones) [78, 79] but in some cases it can be used even low molecular weight alcohols [80], through different types of interactions, *e.g.* electrostatic, van der Waals or hydrogen bond interactions. It is worth mentioning that in recent years the preparation of particles with asymmetric wettability, *i.e.* Janus particles and patchy colloid, is attracting growing technological interest in the preparation of particle-laden interfaces [81–84].

3 Energetic landscape on the adsorption of particles at fluid interfaces

The control of the interfacial self-assembly of particles requires a detailed analysis of the energetic landscape because the final microstructure and dynamics of particle-laden interface results, as was aforementioned, from an intricate balance involving different interactions [85, 86]. For particles attached at fluid interfaces, it is possible to define the energetic balance in terms of the difference between the chemical potentials of the particles at the interface, μ_{int} , and in the bulk, μ_b [3]

$$\Delta\mu = \mu_{\text{int}} - \mu_b, \quad (4)$$

which can be splitted in different contributions

$$\Delta\mu(\phi, \vartheta) = \mu_w + \mu_i(\phi, \vartheta) + \mu_e(\phi, \vartheta), \quad (5)$$

where μ_w , μ_i and μ_e are the components due to the particle wettability, interactions and entropic contributions, respectively. ϕ and ϑ are the volume fraction of particles in the bulk and the interfacial coverage, respectively. μ_w is associated with the effect of the contact angle defined by eq. (3) and μ_e is the unfavorable entropic contribution associated with the reduction of freedom degrees of the particles resulting from their attachment to the interface. μ_i considers the different interactions occurring between particles at fluid interfaces: van der Waals, electrostatic, capillary, fluctuations or hydrophobic. Such interactions emerge from the inter-particle coupling and are strongly dependent on the inter-particle distance, *i.e.* particle density. Attractive interactions favor the attachment of particles at fluid interfaces, whereas the opposite is true when repulsive interactions are considered. It is worth noting that the control of the assembly of particles at the interface is challenging because the inter-particle interactions occur through a discontinuous environment (interface), which defines an asymmetric distribution of the interaction through the different phases [51]. The balance between the aforementioned contributions determines the equilibrium coverage of the interface, ϑ_{eq} .

In this section we briefly describe the role of the most important contributions affecting μ_i . These contributions can be grouped in two different categories [51]. The first group is related to the interactions appearing in bulk systems, which are modified due to the presence of an interface. This is generally called direct interaction and involves electrostatic, hydrophobic and van der Waals interactions. The second group includes the interactions appearing due to the presence of an interface, with the capillary one being its paradigm.

3.1 Direct interactions

The direct interactions occurring between colloids are correlated to the specific nature of the particles. In the following, it is provided a briefly description of the most commonly found in particles systems. There are other types of interactions that can appear as consequence of specific properties of the particles, *e.g.* magnetic or elastic. A detailed discussion on its effect can be found in the work by Oettel and Dietrich [51].

3.1.1 Van der Waals interactions

For particle-laden interfaces, the analysis of the van der Waal interactions is more complex than for particles in the bulk, and can be performed defining an effective Hamaker constant that depends on the volume fraction of particle immersed in the fluid 2 ($f = (1 - \cos \theta)/2$) [3, 50, 87]. Thus, considering an arbitrary interface the effective Hamaker constant A reads as follows

$$A = A_{pf_1} + f^2(3 - 2f)(A_{pf_2} - A_{pf_1}), \quad (6)$$

where A_{pf_1} and A_{pf_2} define the Hamaker constants across fluid 1 and fluid 2, respectively. This allows one to assume that the strength of van der Waals interactions of particles attached at the fluid interfaces can depend on f , *i.e.* of the particle wettability. The average van der Waals interaction between a pair of particles at a fluid interface can be approximated as

$$E_{vdW} = -\frac{A}{12} \left(\frac{a}{R - a} \right), \quad (7)$$

where a defines the inter-particle distance. Recently, Dias *et al.* [88] have pointed out that a similar interaction potential to that provided by eq. (7) accounts for the changes on the growth mechanism of particle domains associated with the asymmetric distribution of interactions appearing in interfaces formed by anisotropic particles [89, 90].

3.1.2 Electrostatic interactions

Electrostatic interactions occur for charged colloids, and are the result of an intricate balance between the screened coulombic repulsion, typical of particles in bulk suspensions, and the long-range dipole-dipole interactions due

to the particles attachment at the fluid interface. The dipolar interactions depend on the nature of the fluid phases across which occur and, thus, they present a clear asymmetry associated with the presence of the interfacial plane [34]. For the part of the particles immersed in the aqueous phase, the dipole is formed by the charges on the particles surface and the counterions dissociated in the bulk, whereas for the part of the particles immersed in the non-polar phase the dipole is formed between surface charges and image charges appearing in the water [50]. The total interaction potential combining the electrostatic and the screened Coulomb interaction reads [91]

$$E_{electrostatic} = \frac{a_1 k_B T}{3r} e^{-\kappa r} + \frac{a_2 k_B T}{r^3}, \quad (8)$$

where a_1 and a_2 are prefactors determining the role of the screened Coulomb potential and the dipolar interaction, respectively. For inter-particle distances long enough ($\kappa r \gg 10$, where κ is the inverse Debye screening length), the role of the dipolar interaction is predominant [92, 93]. It is worth mentioning that electrostatic interactions are linked to the appearance of electrocapillary interactions associated with the deformation of the interface due to the action of electrostatic stresses [50].

3.1.3 Hydrophobic interactions

Hydrophobic interactions present special importance as the size of the particles become smaller. This is explained assuming that in such scale length the molecular details of the solvent and the interface start playing an important role. Thus, the hydrophobic interactions appear as result of the necessity to minimize the unfavorable contacts between the particles and the solvent [94–96]. Despite its importance, no systematic discussion on the role of the hydrophobic interactions in particle-laden interfaces can be found in the literature yet.

3.2 Interactions due to the presence of the interface

The main interactions due to the presence of the interface are the capillary ones. These interactions emerge from the deformation in the direction perpendicular to the fluid interface associated with the adsorption of particles. This originates strong lateral interactions (attractive or repulsive) between colloids. For big particles, gravity is able to induce the deformation of the interface, leading to the so-called flotation forces which decrease strongly with size. These forces are irrelevant when particles are smaller than the interface capillary length because the weight of the particles is too small to induce any significant deformations of the interface. However, for small particles the appearance of other type of capillary forces, the so-called immersion forces, is found. These forces are the consequence of the perturbation of the interface, and present an attractive character over a broad range of length scales. The

capillary interactions can be written as a function of the deformation amplitude of the interface H as follows [97]:

$$E_{capillary}(R) = -12\pi\gamma_{f_1 f_2} H^2 \zeta \frac{r^4}{R^4}, \quad (9)$$

where ζ is a factor depending on the particle orientation. For charged colloids, electrocapillary forces can appear due to differences in the dielectric constant between the two phases, leading also to an the interface deformation comparable to that resulting from the gravity [51, 98].

The above discussion presents so far the most important aspects related to the interactions of particles at fluid interfaces. There are other types of interactions that can emerge from the specific properties of the colloids, *e.g.* elastic, steric or magnetic. However, a comprehensive explanation of the role and origin of the different types of interactions involved in the energetic balance of particle-laden interface is far from the scope of this review, further details on this topic can be found in previous works by Garbin *et al.* [3], Bresme and Oettel [51] and Deshmukh *et al.* [99].

4 Thermodynamics and structural aspects of particle-laden fluid interfaces

It was discussed above that probably the most important feature determining the attachment of particles at fluid interfaces is their surface nature, *i.e.* their HLB. However, particles adsorption presents a main difference with the adsorption of surfactant at fluid interface, which comes from the almost irreversible character of the attachment of particles to the fluid interface [72]. Furthermore, the significant difference existing between the sizes of particles and solvent molecules is an additional difficulty for providing an accurate theoretical description of the thermodynamics behavior of particle-laden interfaces. The aforementioned aspects limit the application of the classical equations of state, *e.g.* Langmuir, Frumkin, etc., in particle monolayers [100]. Hence, the development of new thermodynamics models accounting for the physico-chemical behavior of particle-laden interfaces is required [101, 102].

According to our knowledge, the first thermodynamics model accounting for the behavior of particle-laden interfaces was proposed by Binks [48]. This model was based on the Volmer and van der Waals equations, assuming that each single particle behaves as a surfactant molecule. This leads to consider that the area occupied by a single particle at the interface is equivalent to its geometric area, and consequently it may be expected that the surface pressure $\Pi = \gamma_0 - \gamma$ (with γ_0 and γ being the surface tension of the bare fluid interface and of the particle-laden interface) remains close to zero until the system present hard-sphere behavior (close-packed monolayer). Such contradiction between experiments and theoretical predictions evidences that the role of the interactions occurring at the interface cannot be neglected. Thus, the strong differences existing between particles and common surfactants, especially

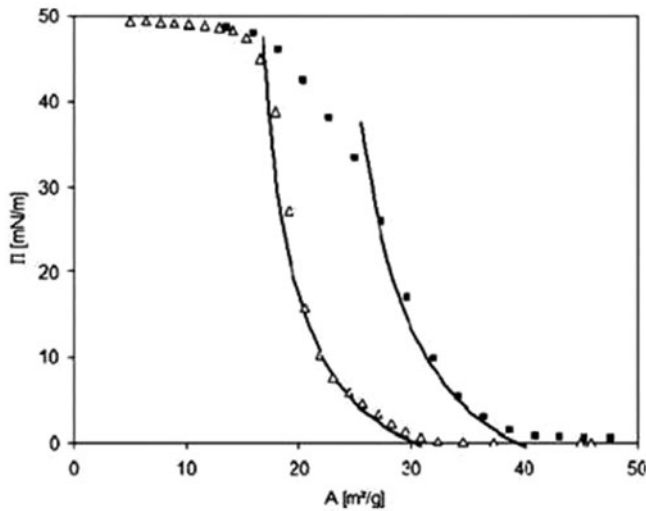


Fig. 4. Comparison between experimental results (symbols) and theoretical predictions (lines) for particle-laden interfaces formed by bare particles (Δ) and steric-stabilized particles (\blacksquare). Reprinted with permission from ref. [102]. Copyright (2006) American Chemical Society.

related to the different length scales involved in their interactions, leads to unrealistic predictions of the dependence of the surface tension on the interfacial coverage, *e.g.* according with the commented model it is expected that only small particles (diameter < 1 nm) at relative high interfacial coverage (50–70% of the total interfacial area) can lead to a significant change of the surface pressure. Some of the limitations of the aforementioned model were overcome by Miller *et al.* [101]. Their description of the interfacial behavior of particle-laden interfaces follows theoretical assumptions similar to previous models used for the description of protein layers [103], including parameters regarding the particle nature. This model provides an expression for the surface pressure isotherm of particle-laden interfaces that reads as follows:

$$\Pi = \frac{k_B T}{\omega_0} \left[\ln \left(1 - \frac{\omega}{A} \right) + \left(\frac{\omega}{A} \right) \right] - \Pi_{coh}, \quad (10)$$

where $\frac{\omega}{A}$ is a term accounting for the coverage of the interface and ω_0 represents the area of a particle. Π_{coh} is the so-called cohesion pressure, which measures the interactions occurring within the particle-laden interface. Even though the above discussed model has been used for a reduced number of systems, the available results foretells a good agreement between experimental results and theoretical predictions, at least for particle monolayers well below of collapse, independently on the nature or size of the particles (see fig. 4).

A more recent model enabling for the description of the thermodynamic behavior of particle-laden interface was proposed by Groot and Stoyanov [104]. They developed a model which included features of the interaction potential on the dependences of the surface pressure on the interfacial coverage, leading to an expression that reads as

follows:

$$\Pi = \frac{4k_B T}{\pi d^2} \left[\frac{byZ}{\lambda} - b_2 y^2 \right], \quad (11)$$

where d represents the distance within the occurring long-range interactions, Z is the compressibility factor [105, 106], $\sqrt{\lambda}$ represents the effective diameter of the particles, y represents the interfacial coverage and b and b_2 are interaction parameters associated with the used potential. This theoretical model has been applied satisfactorily by Deshmukh *et al.* [107] for describing the behavior of soft particles attached at fluid interfaces. It is worth mentioning that the aforementioned models are applicable in most cases to spread monolayers in which the relationship between surface pressure and interfacial coverage is known [78, 79, 105, 108–112].

A complete description of the interfacial behavior of particle-laden interfaces requires some considerations about morphological and structural aspects. For the study of these aspects, it is possible to assume two different approaches: the first one relies on the determination of the particle distribution within the quasi-2D interfaces, *i.e.* the study of the interfacial morphology. The second approach requires the analysis of the position of the particles in relation to the interfacial plane, *i.e.* the determination of the contact angle.

Santini *et al.* [46] study the interfacial morphology of silica nanoparticles decorated with CTAB (hexadecyltrimethylammonium bromide) using Brewster Angle Microscopy (BAM), and conclude that particles hydrophobicity plays a key role on the control of the layer coverage, as was evidenced from the differences in the interfacial textures. Following with the same system Maestro *et al.* [47] showed that the wettability of the particles, and consequently the position of the particles in relation to the interfacial plane, could be also modified by the degree of hydrophobicity of the particles. Similar results were found by Zang *et al.* [56] using silica hydrophobized by chemical silanization. These above results confirm that the importance of the particles wettability in their position in relation to the interfacial plane.

The study of the adsorption of monolayers of silica nanoparticles decorated with palmitic acid at the water/vapor interface showed results in agreement with those discussed above [113]. For particles with the lowest hydrophobicity, isolated aggregates of particles were found at the interface which coalesce as their hydrophobicity is increased, leading to the formation of close-packed particle monolayer. Such behavior is associated with the increase of the interfacial coverage which leads to a sharp decrease of the surface tension with a strong decrease of the surface tension. Figure 5 shows the interfacial textures, surface tension isotherm and thicknesses of monolayers of silica nanoparticles decorated with palmitic acid at the water/vapor interface obtained increasing the concentrations of palmitic acid, *i.e.* particles with increasing hydrophobicity. Santini *et al.* [110], using ellipsometry, showed that the densification of the layer evidenced by BAM was associated with an increase of the layer thickness, *i.e.* of the surface concentration of particles at the interface. This lat-

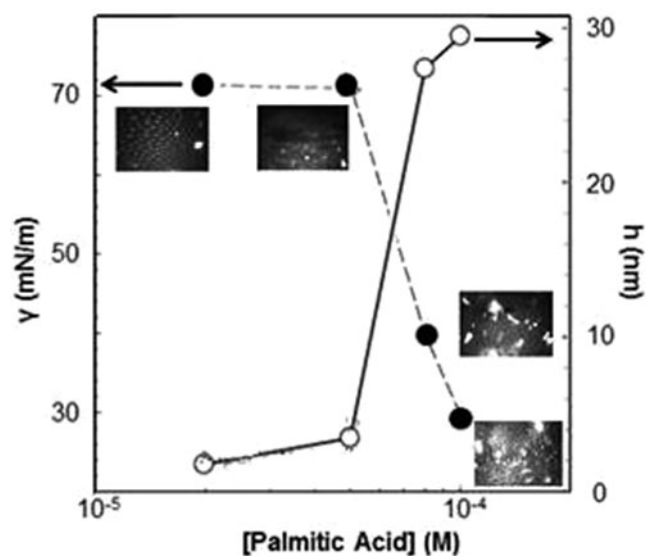


Fig. 5. Interfacial textures obtained by BAM, layer thickness, h , and surface tension for the adsorption of dispersions of silica nanoparticles decorated with different concentrations of palmitic acid at the water/vapor interface. Adapted from ref. [56]. Reproduced by permission of the PCCP Owner Societies.

ter is in qualitative agreement with the results found by the group of Noskov [114–118] for polystyrene sulfate latex micro- and nanoparticles and silica nanoparticles decorated with CTAB at both water/vapor and water/alkane interfaces. The above results allow concluding that the increase of the particles hydrophobicity drives the transition from layer with a lost packing to close-packed particle-laden interfaces.

The main problem when nanoparticles are considered is the impossibility to analyze the packing of each single particle at the interface. However, this is solved when microparticles are studied because their sizes allow characterizing their positions using microscopy analysis. Bonales *et al.* [10] carried out an interesting phase diagram of microparticles of polystyrene sulfate latex at the water/octane interface. Their results agree qualitatively with the above discussion on the densification of the interfacial layers of nanoparticles. However, they were able to observe the appearance of transitions between several phases as the interfacial coverage increases. Such transitions appear independently of the particle size, and only a slight shift of the critical coverage needed for the transition is observed with the change of the particle size. Similar studies were carried out by Parolini *et al.* [119], leading to conclusions in good agreement with those previously obtained by Bonales *et al.* [10]. Studies on binary monolayers of colloidal particles were also carried out by Bonales *et al.* [9], and their results pointed out that the phase behavior of the mixed systems appear as intermediate between that of the individual systems. An interesting way to modify the structure of particle-laden interface is by the mean of physico-chemical stimuli. This was shown by Martínez-Pedrero *et al.* [120] using the magnetic response of superparamagnetic microparticles.

5 Anisotropic particles at fluid interfaces

The above discussion has mostly concerned to the behavior of spherical and nearly spherical particles trapped at fluid interfaces. However, in recent years a growing interest on the study of the interfacial behavior of anisotropic particles has been developed [121, 122]. Asymmetry defines the orientation-dependent interactions at the interface which modify the particle assembly and, consequently, the properties of particle-laden interfaces. Furthermore, the stability of particles trapped at fluid interfaces is correlated to the geometry, existing a critical aspect ratio beyond which particles are not stable at fluid interfaces. In general, elongated particles present less stability at the interfaces than particles having any other geometries. This behavior is ascribable to the higher values of line tension [50]. Loudet *et al.* [123] evidences that the wetting properties, *i.e.* mainly the line tension, is strongly correlated to the aspect ratio of nanoparticles. This has driven an important research for optimizing the organization of rod-like particles and carbon nanotubes at fluid interfaces which requires controlling the surface chemistry of the particles to reduce the line tension below a threshold value about 0.1 nN [50]. Kim *et al.* [124] studied the phase behaviour at interfaces of BaCrO_4 nanorods and evidenced the existence of rich phase behaviour (isotropic, 2D nematic, 2D smectic and 3D nematic) as the interfacial density increases. Similar studies were carried out by Hernández-López *et al.* [125] using carbon nanotubes.

Considering the interactions involved in monolayers of anisotropic particles, it is expected that at short distance the shape can influence the steric and van der Waals interactions. However, the behaviour becomes more complex at long distance mainly due to the effect of the particle geometry in the deformation of the interface, *i.e.* in the capillary forces [50]. Loudet *et al.* [126] studied the assembly of micron-sized ellipsoidal particles at fluid interfaces and found that the asymmetry of interactions occurring at the interface determines the formation of open branched aggregates of particles with a high tendency to the formation of particles chains due to the directionality of the interactions existing at interface [121]. This behaviour contrasts with that found for spherical colloids at fluid interfaces in which the formation of close-packed structures is found [10]. The shape dependence of the interfacial organization of colloids at the interface is explained assuming the different nature of the capillary interactions involved. For non-spherical particles, a long-range capillary interaction of quadrupolar origin, largely exceeding the thermal energy ($k_B T$), accounts for the complex interfacial assembly [126, 127]. It is worth mentioning that capillary interactions in anisotropic particles at fluid interfaces overcome several times than in the case spherical particles [121, 122, 126]. The above landscape evidences that interactions between non-spherical particles is much richer than that found for spherical colloids, leading to a more complex interfacial organization [50].

Deepening on the assembly of anisotropic particles at fluid interfaces, Botto *et al.* [128] showed that the specific

geometry of the particles affects dramatically the energetic landscape and, consequently, the interfacial assembly. This drives the assembly of ellipsoidal particles following a side-to-side configuration to form flexible chains, whereas the assembly of cylinders occurs in an end-to-end configuration that leads to the formation of rigid chains. This is explained considering that capillary interactions are strongly influenced by the geometry of the particles, which can be exploited to obtain interfaces with a broad range of properties.

An additional aspect to take into account when the assembly of anisotropic particles at fluid interfaces is considered is the preferential orientation. The existence of a preferred direction for the adsorption of colloidal particles at fluid interfaces was demonstrated by Isa *et al.* [129] using contact angle measurements of polymeric dumbbells in which each lobe presents a different wettability for the phases. The results evidence that the preferred orientation for the adsorption of dumbbells was in tilted configuration. In a similar way, the adsorption and assembly of patchy colloids present a preferential orientation which is associated with the opening angle of the patches [130–132].

It is worth mentioning that the progresses on the understanding of the interfacial organization and properties of assemblies of anisotropic particles is more difficult than for spherical particles, mainly because of the complicated fabrication process of anisotropic shapes particles under controlled conditions.

6 Dynamics of particles at fluid interfaces

The understanding of the dynamics of particle at fluid interfaces requires considering both the inter-particle and the particle-solvent interactions. Therefore, the motion of colloids attached to fluid interfaces is strongly dependent on the hydrodynamics constrains associated with the presence of the surrounding fluid, which determine, in most of the cases, the time-scales governing the behavior of particle attached at fluid interfaces [133–139].

At the shortest time, the fluid phase presents a compressible-like behavior and the colloidal motion leads to a density fluctuation similar to a sound wave, with its characteristic time being defined by $t_s = R/c_s$, where R and c_s represent the radius of the colloid and the velocity of sound, respectively. The time-scales involved in this motion are extremely short around 10^{-1} ns, and thus it cannot be measurable with most of conventional techniques.

A second time, t_h , is associated with hydrodynamics interactions. The colloidal motion origins a transverse momentum diffusing away from the particles. The originated velocity field induces a drag force between the particles. The time-scale involved in this process is around 10 ns that is equivalent to the time required for the transverse momentum to diffuse along the typical inter-particle distance which is comparable to the diameters of the colloids. Coupled with the motion due to the hydrodynamics interactions appear other dynamics associated with the decay of the initial velocity of a colloid. These are a consequence of the effects provoked on the particles by the

action of time-dependent velocity fields appearing in fluids due to particle motion. The time-scales of these dynamics are governed by the diffusion coefficient of the transverse momentum of the fluid.

When colloids are considered, they present a diffusion-controlled motion with a typical diffusion constant defined by $D_0 = k_B T/g$, where g is the Stokes friction coefficient. The characteristic time for the motion of colloids at the interface along a distance similar to their radius appears in the range 10^{-3} –1 s. This evidences clearly the separation between the diffusion of colloids and other motions. Thus, it is possible to assume that the motion of colloids can be considered as an uncorrelated Brownian motion in the long-time limit. However, it is worth mentioning that this approach presents some limitations because the diffusion of each single colloid depends significantly on the configuration of its neighbor due to the occurring interactions.

The analysis of the particles trajectories at fluid interfaces by videomicroscopy provides information related to the dynamics involved in the particle-laden interface. This information can be obtained from the calculation of the mean square displacement, MSD ($\langle \Delta r^2(t) \rangle$), which is related to the diffusion coefficient, D , and the characteristic length of the translational motion, as follows:

$$\langle \Delta r^2(t) \rangle = 2dDt^\alpha, \quad (12)$$

where α is a scale exponent. Considering particle monolayers with low coverage, it can be expected a linear dependence of the MSD on t , and the characteristic diffusion time can be easily obtained according to eq. (12) from the slope of the representation [6, 140, 141]. However, the densification of the monolayers drives the transition to a more complex dynamics regime, and a clear differentiation between the short-time and long-time dynamics appears. This difference is characterized by a change of the slope which can be explained assuming that in the short-time limit, particles diffusion is constrained to the region limited by their closer neighbor, leading to a short-time self-diffusion coefficient defined as follows:

$$D_s = \lim_{t \rightarrow 0} \frac{\langle \Delta r^2 \rangle}{4t}. \quad (13)$$

The diffusion coefficient in the short-time limit decreases as the surface coverage, ϑ , of the particle-laden interface increases as result of the interactions $D_s = \alpha D_0(1 - \mu\vartheta)$, where μ is a parameter depending on the interactions [142]. In the long-time limit, the collective motion of particles start to play a role on the dynamics of the particle-laden interface and it is possible to define a diffusion coefficient in the long-time limit as follows:

$$D_m = \lim_{t \rightarrow \infty} \frac{\langle \Delta r^2 \rangle}{4t}, \quad (14)$$

The process defined by the long-time dynamics response on particle-laden interfaces can be rationalized by particles escaping from their cage, delimited by their nearest neighbors, the so-called α -relaxation [143–145]. When

the interfacial density is high, the inter-particle repulsions leads to arrested dynamic within the experimental accessible time windows. Under these conditions there are no analytical results and the results are analyzed in terms of the harmonically bound independent Brownian oscillator (BHO), in which particles behavior obeys to the Langevin equation including an elastic force [146, 147]

$$m \frac{dv}{dx} = -gv + F(t) - kx, \quad (15)$$

with m being the mass of a particle, v represents its velocity and k the characteristic force constant of the elastic force acting on the particle. $F(t)$ represents the random force. Considering the overdamped limit, and neglecting the role of the inertia, the model leads to the following solution [143, 144]:

$$\langle \Delta r^2(t) \rangle = 2d\delta^2 \left[1 - e^{-D_0 t / \delta^2} \right], \quad (16)$$

where $\delta^2 = k_B T / k$. The characteristic time is defined as $t_{BHO} = \delta^2 / D_0 = g / k$. Several ad hoc corrections have been introduced to the above equation in order to describe the dynamics of interacting Brownian particles. A more complete description is given by the following equation that accounts for a non-exponential character of the decay [148, 149]:

$$\langle \Delta r^2(t) \rangle = 2d\delta^2 \left[1 - e^{-(D_0 t / \delta^2)^c} \right] \left(1 + \frac{D_0 t}{\delta^2} \right). \quad (17)$$

Equation (17) introduces a stretching exponent c , and a term accounting for long-term dynamics of particles escaping from particles groups, which recovers the linear dependence on time. The stretching exponent is a fitting parameter, assuming values lower than 1 and accounts for the width of the spectrum of relaxation time.

For monolayers showing a solid-like character, the above model is no longer applicable, and it is needed to develop a new model. The Overdamped Bead-Spring model (OBS) accounting for particle dynamics under high density conditions reads as follows [150, 151]:

$$m \frac{dv_i}{dt} = -gv_i(t) + F_i(t) - k \sum_j^{nn} [u_j(t) - u_i(t)], \quad (18)$$

where $u_i(t)$ is the displacement of the particle i at time t , and nn is the number of nearest neighbors of particle i . The high density of particles existing in solid-like monolayer hinders the escaping dynamics of particles from the groups, and thus the MSD does not present any linear increase at long times. The solution of the above model reads

$$\langle \Delta r^2(t) \rangle = \frac{2dk_B T}{kN} \sum_b \frac{1}{L(q_b)} \left[1 - e^{-kL(q_b)t/b} \right]. \quad (19)$$

The above equation only considers the interaction between closer neighbors. $L(q_b) = \sum_j^{nn} [1 - \cos(q_x n_j)]$ is the lattice

factor, with q_b being the b -th wave vector of the relaxation mode q , and n_j takes into account a vector pointing from the point i of the lattice to its closer neighbor j . The OBS model leads to a similar slope in the MSD than the BHO one in the initial stages, and tends to a limit value defined by

$$\lim_{t \rightarrow \infty} \langle \Delta r^2(t) \rangle (t \rightarrow \infty) = \frac{2dk_B T}{kN} \sum_b \frac{1}{L(q_b)}, \quad (20)$$

The long limit depends on both the strength of the harmonic force and the lattice factor.

7 Rheological response of particle-laden fluid interfaces

This section is devoted to explain the response of particle-laden interfaces against mechanical perturbations, paying special interest on the relaxation mechanisms of micro and nanoparticles [6, 40, 41, 152–155]. A deep understanding on the mechanical properties of particle-laden interfaces, hence, might be a key to understand and improve many technological applications associated with the interaction of particles and interfaces, *e.g.* phase transfer catalysis, encapsulation, enhanced oil recovery or emulsification and foaming [156].

7.1 Dilational rheology

Dilational rheology experiments provide information on the changes induces on the surface tension due to the modification on the interfacial area. Thus, it is possible to assume that infinitesimal changes of the area of the interface, $\delta A(t)$, due to an uniaxial stress leads to a time-dependent change of the surface pressure defined by $\delta \Pi(t)$, which could be defined as follows [157]:

$$\delta \Pi(t) = \Pi(t) - \Pi_0 = \frac{\partial \Pi}{\partial A} \delta A = -\varepsilon(t)u(t) \quad (21)$$

with $\varepsilon(t) = -A_0(\partial \Pi / \partial A)_T$ representing the time-dependent dilational modulus. The above equation is a general time-dependent response function, where the surface stress $\delta \Pi$ results from a perturbation given by a compression strain $u(t) = \delta A / A_0$. For fluid films at equilibrium, the dynamic modulus is equal to the Gibbs elasticity ε_0 :

$$\varepsilon(t) \rightarrow \varepsilon_0 = \Gamma \left(\frac{\partial \Pi}{\partial \Gamma} \right)_{eq}, \quad (22)$$

where $\Gamma = 1/A$ is the surface concentration. For small-amplitude oscillatory deformation with frequency ω , the complex modulus reads as

$$\varepsilon(\omega) = \varepsilon'(\omega) + i\omega\kappa(\omega). \quad (23)$$

where the real part $\varepsilon'(\omega)$ corresponds to the storage modulus and the imaginary part $\varepsilon''(\omega) = \omega\kappa(\omega)$ is referred to

the loss modulus, being κ the interfacial dilational viscosity. The definition of the viscoelastic dilational modulus allows expecting modifications either on the adsorption state of the particles at the fluid interface or on the structure of the interface as a consequence of the stress induced by the deformation. Different relaxation dynamics characterized by different time-scales can appear as response to a dilational perturbation of the interfacial area [109, 158].

Despite the big number of experimental and theoretical studies dealing with the response of particle-laden interfaces against dilational stresses, there are many aspects that remain unclear, especially when theoretical predictions and experimental results are compared [6, 11, 101, 109].

On the best of our knowledge, the first study dealing with the response to dilational stresses of particle-laden interface was carried out by Miller *et al.* [101]. They studied the relaxation of particle-laden films on the basis of theoretical models similar to those generally used for describing the interfacial behavior of proteins and proteins-surfactant systems [159, 160]. This framework provides a description of the mechanical response of particle-laden interfaces on the bases of the information obtained from their adsorption isotherms. However, this study remains as a mainly theoretical one and no further advancements on the application of the aforementioned model to experimental results have been performed yet.

As was already mentioned, the attachment of particle to fluid interfaces is strongly correlated to their wettability, thus it is expected that this parameter may present an important effect on the dilational response of particle-laden interfaces. Safouane *et al.* [161] explored the dilational response of fumed silica nanoparticle monolayers at the water/vapor interface using capillary waves in the frequency range 200–990 kHz and found that the rheological response was influenced by the interfacial morphology. However, they carried out that independently of the hydrophobization degree of the nanoparticles and the surface coverage, the elastic component of the response was higher than the viscous one and increases with the hydrophobicity of the particles due to their favored incorporation to the interface. This rigidification of the film associated with its densification is explained considering an enhancement of the inter-particle interactions as was pointed out by Zahn *et al.* [162]. When the loss modulus is analysed, no dependences on the wettability or interfacial concentration of the layer were found.

Zang *et al.* [45] extended the studies by Safouane *et al.* [161] to the low frequency range and found the existence of a relaxation process on a time-scale comparable to 1000 s. This process was associated with the reorganization of particles at the interface and becomes faster as the hydrophobicity of the nanoparticles decreases. This could be explained assuming the smaller surface coverage of the interface as the particles hydrophobicity decreases, thus it is expected a favoured reorganization of the particles at the fluid interface due to the reduced steric hindrance. Furthermore, they found that spread layers present lower rigidity than compression one. This is explained consider-

ing that the latter present non-equilibrium arrested states that lead to the emergence of additional relaxation processes to the particle-laden interface [45, 163].

Beyond silica nanoparticles, the rheology of latex micro-particles spread at fluid interfaces have been widely studied in recent years [114, 115, 155, 164]. Kobayashi and Kawaguchi [164] studied latex particles spread at the water/vapor interface and found that the particle-laden interface presents a viscoelastic behavior independently of the strain rate. In addition, they found a certain hysteresis that is associated with the lost connection between particles in the monolayers. The increase of the storage and loss moduli was found with the densification of the monolayer. However, once the coverage reaches a critical value (at $\Pi \sim 15$ mN/m), both start to decrease steeply. This is explained considering the possible buckling of the monolayer that distorts the 2D packing of the monolayer. From the frequency dependences of the storage and loss moduli the transition from a mainly fluid-like behavior to a solid-like one was found, which is correlated to the structural scenario found by Bonales *et al.* [10]. Deepening on the correlations between the dilational response and structural richness of the particle-laden interfaces, del Rio *et al.* [165] found that the dilational modulus presents an important correlation to the region of the phase diagram studied, with the storage modulus being always higher than the loss modulus. For low surface pressure, the storage modulus increases with the monolayer densification whereas the loss modulus remains constant at values close to that of the water. This could be explained on the basis of the important role of the repulsive electrostatic interactions between particles. The storage modulus presents a sharp increase till values around 350 mN/m. This results in the formation of close-packed a monolayer as was evidenced by BAM imaging. When the electrostatic repulsion is so high, the storage modulus can reach values until 600 mN/m. This is explained assuming the presence of a small number of defects in the close-packed monolayer. In agreement with the result by Kobayashi and Kawaguchi [164], del Rio *et al.* also found a decrease of the storage and loss moduli for the highest surface pressures due to the breaking of the 2D packing of the interface. Qualitative similar results to those found for water/vapor interfaces were found when latex monolayers at water/oil interface were considered [114, 115]. It is worth mentioning that particle-laden interface present a relatively small range of linearity on their dilation response, which makes necessary to apply low strains deformations on the studies of particle-laden interfaces [155].

The dilational rheology of monolayers formed by the mixture of particles and surfactant has been studied in more detail than that of monolayer formed only by nanoparticles. This can be in part ascribed to the versatility of the use of surfactants for modifying particles wettability [11]. It is expected that the interaction of two components bearing oppositely charged in solution can presented important effects on the interfacial properties of such mixture, *e.g.* the appearance of synergetic effects on the surface tension decrease due to the adsorption of the complexes formed in the bulk [166–169].

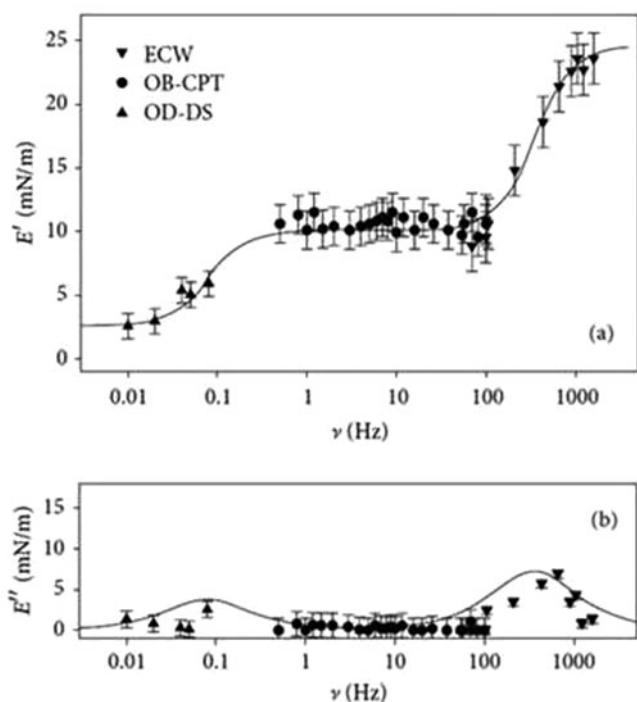


Fig. 6. Wide range dilational response of silica nanoparticles (1 wt%) decorated with CTAB (0.05 mM) at the water/vapor interface as were obtained combining different experimental techniques. (a) Dependence of the elastic modulus on the deformation frequency. (b) Dependence of the viscous modulus on the deformation frequency. Reproduced from ref. [109] with permission from The Royal Society of Chemistry. Copyright (2011).

However, this is not always true as was evidenced by Ravera *et al.* [78] studying mixtures of silica nanoparticles and CTAB. Other noticeable effects of the interactions were found in the dilational response in the low frequency limit (0.005–0.2 Hz): 1) higher elasticity of the particle-laden interface than the monolayer of pure surfactant and 2) strong dependence of the viscoelastic response on frequency. Furthermore, it was found a stronger effect of the particles adsorption at the water/oil interface than in the water/vapor interface. A more detailed study, concretely in a broad frequency range (10^{-3} – 10^3 Hz), of the rheological response of the aforementioned system evidenced two different relaxation processes of the interfacial layer related to the diffusion of the particles from the bulk to the interface and the reorganization of adsorbed material at the interface [108, 109] (see fig. 6). The results were described in terms of a mixed rheological mechanism considering a diffusion process and arbitrary kinetics occurring at the interface.

There are other works dealing with the study of the rheological response of mixtures formed by CTAB and silica nanoparticles which have evidenced the role of the complex balance of interactions in the control of the rheological response. The most important interactions can be ascribed to the CTAB depletion, the electrostatic and hydrophobic interaction controlling the wettability of parti-

cles and the interactions between particles in the bulk and at the interface [46, 47, 170].

It is also important to consider the role of the interfacial aging on the mechanical response of particle-laden interfaces. This leads frequently to an increase of the dilational elasticity for layers at both water/vapor and water/hexane interfaces [108, 116, 117]. Despite this rigidification process induced by the aging, no changes on surface tension was evidenced which is ascribable to the irreversible attachment of the particles at the interface. The rigidification results from the formation of solid-like layers as was evidenced by BAM images [116]. The elastic modulus found for solid-like monolayers is comparable to those found in latex monolayers [164, 165]. This result well agrees with the results found in order systems by Whitby *et al.* [171] and by Santini *et al.* [108].

Other particle-laden interfaces that deserve special attention are those formed by lipid and nanoparticles. These systems present big interest due to their usefulness as model for studying the potential toxicity of inhaled particles. However, a detailed discussion of the rheology of such systems is far from the scope of this review [25, 26, 172–180].

7.2 Shear rheology

Shear deformations are completely decoupled from any other interfacial mode, *i.e.* their amplitude and time evolution are independent [181, 182]. For a typical in-plane deformation it is possible to provide a definition of the shear elasticity as the constant of proportionality between the applied strain (u_{xy}) and the stress (σ_{xy}). It is expected that the description of “solid” films can be carried out in terms of a Hookean behaviour characterized by the aforementioned proportionality: $\sigma_{xy} = G u_{xy}$. For totally “fluid” films, the behaviour is described by its viscous character: $\sigma_{xy} = \eta du_{xy}/dt$, where du_{xy}/dt defines the strain rate and η the interfacial viscosity. The viscoelastic parameters (G, η) are increased by the presence of attractive interaction between the species at the interface. This can be explained considering that part of the energy is needed to overcome the interaction, allowing the flow of the surface elements. Considering an oscillatory deformation, it is possible to define the complex shear modulus G^* as follows:

$$G^*(\omega) = G'(\omega) + iG''(\omega) \equiv G' + i\omega\eta \quad (24)$$

with G' and G'' representing the storage and loss moduli, respectively. For small-amplitude oscillatory deformations with a fixed frequency ω it is possible to correlate the loss modulus and the viscous friction $G'' = \omega\eta$, where η is the interfacial shear viscosity. The understanding of the response against shear perturbation of particle-laden interfaces has been strongly developed in the last years due to their recognized impact in many aspects involving these systems [6, 12]. This has fostered the research on this field to provide a detailed explanation about the correlation existing between the response against shear of particle-laden interfaces and the morphology of the layers. It is

worth mentioning that the interactions between particles are the main parameters affecting the shear response of the monolayers [183].

One of the first studies dealing with the characterization of the shear response of particle-laden interfaces was carried out by Cicuta *et al.* [184]. They studied monolayers of polystyrene latex ($3\ \mu\text{m}$ of diameter) at the water/decane interface and found that, in contrast with that found when the dilational response was analysed, the layers present a mainly viscous character with $G'' > G'$. This is different to that found for β -lactoglobulin layers which present a mainly elastic behaviour due to the possibility to be deformed and compressed as response to the compression. Furthermore, it was found a sharp increase of the viscoelasticity of particle-laden interface for surface coverages overcoming the 75–80% of the total area, which is associated with a jamming of the 2D film. It is worth mentioning that the differences in the existing interactions between particle-laden interfaces and particles in the bulk define the different shear behaviour between particle-laden interfaces and their bulk counterparts [185].

Reynaert *et al.* [186] explored the correlations existing between interfacial structure and rheological response in particle-laden interfaces and found that an interfacial aggregation leads to a shear response similar to that found in the bulk systems, which confirms the important effect of the interactions in the control of the rheological response. This was later confirmed by Wijmans and Dickinson [187] by Brownian dynamic simulations.

Imperiali *et al.* [188] studied the effect of the interfacial coverage on the shear response of asymmetric particles as graphene oxide, and found that the different freedom of the particles to reorganize at the fluid interface plays a central role on their shear response. Thus, at low fraction of coverage, the interface presents a reminiscent behaviour of 2D-platicized systems, whereas close-packed monolayers evidenced a perfectly elastic behaviour. Similar dependences of the shear response on the interfacial coverage were found by Barman and Cristopher [189]. They found a transition from shear thinning behaviour to yielding one with the increase of the interfacial density. This is explained on the bases of the differences in the mechanism involves in the dissipation of the viscous stresses. Furthermore, the response becomes non-linear with the increase of the surface coverage; with the viscoelastic modulus following a power law dependence on the surface coverage [186].

Deepening the role of the particle morphology on the interfacial shear response, Madivala *et al.* [190] studied ellipsoidal polystyrene particles at both water/decane and water/vapor interfaces. They found that the different strength of the electrostatic interactions determined different interfacial structures. In the case of water/decane interfaces, particles arrange forming structures in which individual particles coexist with linear aggregates, whereas at the water/vapor interface particles are organized forming flower-like aggregates. The differences in particles organization leads to strong differences in the response against shear of the particle-laden interface, which is an additional evidence of the correlations existing between the self-assembly of particles at the fluid interface and the

mechanical response of particle-laden interfaces. In contrast to that found for spherical particle, the response of asymmetric particle monolayers at the water/decane interface to shear deformation is mainly elastic, with a viscoelastic modulus increasing with the packing modulus. When particles at the water/vapour interface are considered, lower values of the shear elasticity were found. It is worth mentioning that the elasticity of ellipsoidal particles at fluid interfaces is relatively high, even when the surface coverage is small, which differs from the above discussed behaviour when spherical particles are considered [184]. These differences between ellipsoidal and spherical particles are associated with differences on the interfacial relaxation mechanisms [191]. Ellipsoidal particles present a buckling transition, which does not appear for spherical particles, when the interfacial coverage is high. Such differences on the rheological response are associated with the richness of the interfacial phase behaviour of non-spherical particles. The complex balance of interactions given the particular aggregation pattern at fluid interfaces governs the rheological response of particle-laden interfaces, *e.g.* the shear modulus of colloidal crystals formed by paramagnetic particles was found to increase with the strength of the inter-particle repulsion [162].

The role of particles morphology on the shear response was also studied by Brown *et al.* [192] using non-spherical particles with different aspect ratio. In all the cases, shear thickening phenomena were found. However, the increase of the asymmetry of the particles leads to a decrease of the threshold coverage in which interfacial particles jamming occurs. Furthermore, asymmetric particles can present a behaviour that may be reminiscent of the formation of non-equilibrium trapped layers, affecting the shear flows at the interface. This is correlated to the particle charge and the interfacial coverage [193, 194].

Another important parameter affecting the rheological response of particle-laden interface is the roughness of the particle surface [195]. The roughness presents different effects on the rheological response of the particle-laden interface depending on the interfacial coverage. For low density monolayers, the surface roughness reduces the shear viscosity, whereas the opposite is true when monolayers in the vicinity of the jamming transition are considered. This is explained as result of the inter-particle friction as was demonstrated by Brown *et al.* [192], which plays an important role for emulsion behaviour [196]. The importance of the heterogeneity of particle surface for its trapping to fluid interfaces have been recently demonstrated by Zanini *et al.* [197]. They showed that surface roughness can lead to the attachment of particles in metastable positions due to the pinning of the contact line, with such metastable positions being able to be far from the real equilibrium position. Therefore, the surface roughness may induce that hydrophilic particles behaves as hydrophobic ones and the opposite situation, providing the bases for stabilizing water in oil or oil in water emulsions in the same water-oil mixture using only a single type of particles.

As can be expected from the above discussion, particle wettability plays also a relevant role on the rheological response of particle-laden interfaces due to its im-

portance for the attachment of particle to the fluid interface [161]. Safouane *et al.* [161] compared the shear moduli of monolayers of fumed silica with different hydrophobicity degree at the same coverage, finding the increase of both the storage and the loss moduli with the particle hydrophobicity. The behaviour of particles with low hydrophobicity was found mainly elastic, whereas the increase of the hydrophobicity leads to a mainly viscous behaviour with a gel point ($G' = G''$) found for particles with contact angle around 90° . The effect of the hydrophobicity on the aforementioned system was extended by Zang *et al.* [45, 52, 198]. They found that the storage modulus does not present any dependence on the strain amplitude for low values of the strain amplitude, with the storage modulus being almost two orders of magnitude higher than the loss modulus. The monolayers present a melting transition when the strain amplitude overcomes a certain value (yield stress), with the loss modulus becoming maximum and the storage modulus dropping. When the deformation frequency is small a mainly viscous behaviour was found, becoming mainly elastic for high frequencies. The crossover appears for frequencies close to those in which G'' is maximum. This behavior is reminiscent to that observing in 3D soft solids that is the consequence of the decrease of the characteristic time of the structural relaxation due to the increase of the strain-rate amplitude [199]. Similar reminiscence was also found in the quasi-linear dependence of the relaxation time on the shear rate. An interesting aspect of this monolayer is its self-healing character upon the stress release. This shows an important dependence on the coverage and wettability of the particles, with wettability playing a critical role in the control of the yield and melting stresses of particle-laden interfaces. Similar behavior to the above discussed were found independently by Vandebriel *et al.* [200].

Beyond the understanding of the response against shear of the formed layers, the study of the evolution of the rheological properties during the formation of the layers present certain interest [201]. The study of the adsorption kinetics of silver nanoparticles (10–50 nm of diameter) at the water/toluene interface by rheological measurements evidences the increase of G' and G'' with time. This is compatible with a densification during the equilibration process of the layer. The equilibrium films present a mainly elastic behavior and the negative slope found for the dependence of G'' on the deformation frequency evidence the 2D glassy nature of the adsorbed layers. Furthermore, a significant dependence of the response on the strain amplitude was found in this system. Using strain sweep measurements shear thickening phenomena in G'' were found at large strain amplitudes, whereas no dependence of G' on the strain amplitude were found until the shear thickening point. This shear thickening is described by a power law with relation 2:1 on the exponents of the storage and loss moduli. For gold nanoparticles at the water/vapor interface a rather different behavior was reported [36, 37, 202, 203]. The shear response of the above mentioned system presents a gel-like behavior characterized by a strain induced softening. Furthermore, the rheological response was independent of the applied strain

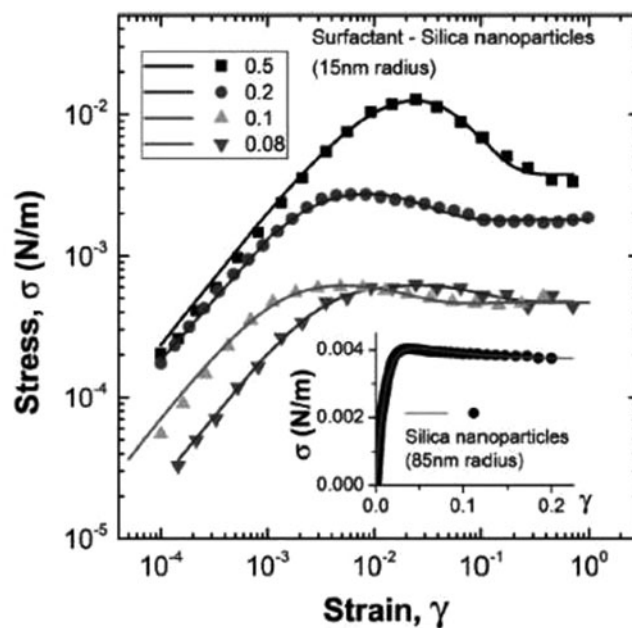


Fig. 7. Experimental (lines) and calculated (symbols) dependences of the interfacial shear stress σ on the amplitude of strain γ at a constant frequency $\omega = 0.628 \text{ rad s}^{-1}$ for silica nanoparticles decorated with CTAB, using different concentrations of surfactant C_s (expressed in mM). Reproduced from ref. [202] with permission from The Royal Society of Chemistry. Copyright (2017).

until a threshold value close to 0.1%. Once the strain overcomes the aforementioned threshold the storage modulus drops. The dependence of the viscoelastic moduli on the interfacial coverage for this system can be described in terms of a power law with an exponent assuming a value around 0.65, which is reminiscent of a percolating system [158, 204, 205].

Minor attention has been paid so far to the shear response of mixtures of particles and surfactants at fluid interfaces. Maestro *et al.* [199] explored the effect of the surfactant concentration on the shear rheology of silica nanoparticle-laden interfaces. Strain-sweep experiments shown in fig. 7 revealed that silica nanoparticles trapped at air-water interface form a 2D solid state with amorphous order. Further, they proposed a theoretical model to describe how this solid-like state deforms under a shear strain ramp up to and beyond a yielding point which leads to plastic flow [200]. The model accounts for all the particle-level and many-body physics of the system: non-affine displacements, local connectivity, and its evolution in terms of cage-breaking, and inter-particle interactions mediated by the particle chemistry and colloidal forces. In addition, the yielding behavior of surfactant-decorated silica nanoparticles has also been studied by large-amplitude oscillatory rheology [201].

The interfacial interaction of lipids and silica with different degrees of hydrophobicity was analyzed by Mass *et al.* [206]. They found two-step adsorption kinetics at the water/oil interface. The first step appears in time-scale around 1 hour. During this step G' increases due to the

formation of an elastic layer presenting high cohesion. The second step is much slower and characterized by a slow increase of both G' and G'' due to the accumulation of material at the interface. This continues until the steady state is reached. The values of the storage and loss moduli of the layers are several orders of magnitude above those expected for pure surfactant monolayers in agreement with other studied [161, 207, 208].

8 Active particles at fluid interfaces

In general, active colloids use as external input for their autonomous motion energy obtained from the environment [209–221]. There are several propulsion mechanisms for these materials, among them chemical reactions and external fields are probably the most extended [220]. Many of that is known about active particles in relation to their bulk behavior. However, the understanding of the effect of its confinement at interfaces presents particular interest because the restrictions associated with the reduced dimensionality can drive significant differences on their autonomous motion [220]. In the following some aspects of the interfacial behavior of active colloids trapped at fluid interfaces will be discussed.

The main difference associated with the attachment of particle to fluid interface is that the interface constrains the particle motion to 2D. Thus, the motion of particles in the direction perpendicular to the interface is forbidden, and the motion along the interface leads to drag forces similar to those appearing for the particles in the bulk [222]. When water/vapor interfaces are considered, the vapor phase presents an important role on the confinement effects because it induces an almost negligible stress tangent to the interface. This is similar to that happening for active particles moving in an unbounded fluid presenting a plane of mirror symmetry which enables for the application of similar propulsion mechanisms for the active particles at the interface than in the bulk [223–225].

Another important aspect is associated with the hydrodynamic flows that accompany the particles. These are strongly dependent on the proximity of particles to the fluid boundaries. They enable the hydrodynamic coupling between translation and rotational motions which allow particles to move linearly due to the action of torques associated with external fields, *e.g.* electric or magnetic [221, 226]. These torques lead to a rolling motion of the particles along the fluid interface describing the so-called colloidal moonwalk [221]. In general, the motion of active particles at fluid interface occurs with the particles rotating toward the viscous fluid [227].

The role of capillary forces on the motion of particles attached to fluid interfaces is essential, constraining furtherly the rotation of particles. For self-phoretic colloids, capillary forces enhance almost one order or magnitude the persistence length of their swimming motion. This is associated with a reduction of the rotational diffusion due to the enhanced drag mediated by thermally activate fluctuations of the contact line [228, 229]. Furthermore, capillary forces also limit the rotation of particles around the two axes parallel to the interface, thus

the motion is strongly correlated to the initial orientation of particle which is correlate to the surface properties of particles [230].

The motion of active particles at fluid interfaces can be modulated by the surface tension and the parameter allowing its modification, *e.g.* temperature or surfactant concentration. This enables for the motion of a particular types of active particles, the so-called Marangoni surfers [231, 232]. Marangoni surfers use energy originated by chemical reactions or external energy inputs to induce surface tension gradient at the interface. This leads to forces and torques that provide the bases for a high speed motion of particles to regions of high surface tension. Thus, particle motion is accompanied by Marangoni flows that induce interactions between particles and the system boundaries [233]. These interactions can be either attractive or repulsive, leading to the formation of assemblies and particle swarms. Further details on the behavior of active colloids trapped at fluid interfaces can be found in the work by Fei *et al.* [220] and references therein.

9 Particles at fluid interfaces on the stabilization of dispersed system

The stabilization and properties of dispersed systems (foams, emulsions and thin films) is considered to be closely correlated to the interfacial and mechanical properties of single interfaces, especially when particles are used for their stabilization. This is because particle-laden interface allows hindering, at least partially, the processes determining the destabilization of dispersed systems, mainly emulsions and foams, *e.g.* creaming (or sedimentation), flocculation, coalescence, and Ostwald ripening [8, 14, 234–237]. When the stabilization of dispersed systems is considered, the stability of the liquid film formed between drops or bubbles is essential. An important aspect of this stability is related to their mechanical properties, the adsorbed film must be able to dampen external perturbations in order to avoid the destabilization of the dispersed systems and its breaking.

Particle are very interesting for the stabilization of drops and bubbles, because, as was discussed above, they can remain irreversibly trapped at the fluid interface leading to particle-stabilize foams and Ramsdem-Pickering emulsions [42, 43, 66, 238]. Especially interesting are those systems in which drops or bubbles are highly covered. Several authors have confirmed the role of this latter aspect on the stabilization of dispersed systems [193, 239, 240]. Their results showed that beyond the importance of the mechanical stability of the particle-laden interface, the steric hindrance associated with the formation of a sufficiently dense layer is essential for stabilization purposes. Stratford *et al.* [241] and Maestro *et al.* [242] showed that jammed particle-laden interfaces present the highest efficiency on the stabilization of emulsions and foams, respectively which agrees with the results of the studies of dispersed systems stabilized by silica nanoparticles carried out by Frith *et al.* [243]. This latter showed that the formation of a close-packed particle

layer is mandatory to confer rigidity to drops or bubbles, favoring the stabilization processes. Jamming of particle-laden interface arrests the interfacial tension driven coarsening, enhancing the stability of the interfaces. It is worth mentioning that there is no linear correlation between the solid concentration and the stabilization of dispersed systems. The rheological properties of the particle-laden interface are also influenced by the coverage as was above discussed. Thus, the viscoelastic properties of the layers play also an important role on the stabilization of the foams and emulsions because they control the film thinning processes. The importance of the mechanical properties was confirmed in the studies by Sullivan and Kilpatrick [244]. They showed that the stabilization of the dispersed system was enhanced by particles forming rigid and stagnant films. Therefore, it is possible to assume that the understanding of the inter-particle interactions is essential for controlling the stabilization of dispersed systems [245]. This is evidenced because particle bridging can lead to a further stabilization of foams and emulsions, especially when the coverage is small. These conditions allow the direct aggregation of drops or bubbles causing stable flocs. These interfaces in close contact can lead to the formation of long regions of particle bridges, the so-called particle zips. This leads to the formation of networked monolayers that provide additional stabilization to the dispersed systems [240, 246].

From the above picture, it is clear that the presence of particles attached to fluid interfaces is essential to prevent drops and bubbles coalescence, enabling the stabilization of emulsions and foams. It is worth mentioning that the morphology and droplet size distribution is governed by dimension and contact angle of particles at the fluid interface. The stabilization requires a partial wettability of the particles by both phases. Considering particles at an arbitrary fluid interface, two different situations can appear. For relatively hydrophilic particles ($\theta < 90^\circ$) the formation of oil(air)/water dispersions is preferred for mixtures containing equal volumes of both fluid phase. The opposite is true for hydrophobic particles ($\theta > 90^\circ$). Thus, $\theta = 90^\circ$ must be considered as an inversion point which is defined by the equal affinity of the particles for both fluid phases [238]. It is worth mentioning that the stability of foams and emulsions can be controlled by the addition of surfactants that can favor the ability of particles to reside at the fluid interface [247]. This is understood clearly from the results by Binks *et al.* [248]. They found that for emulsions stabilized by silica nanoparticles and a bicationic surfactant the concentration of surfactant allows tuning the transition between different types of emulsions as a consequence of the hydrophobization degree of the nanoparticles. The study of this phenomenon was extended by measurements of the contact angle of particles at the fluid interface as function of the surfactant concentration, and they found that, for low surfactant concentrations, particles remain hydrophilic with contact angle lower than 90° stabilizing oil in water (o/w) emulsions, whereas for intermediate surfactant concentrations the particles become hydrophobic ($\theta > 90^\circ$) and water in oil emulsions (w/o) were favored. For the highest surfac-

tant concentration, a rehydrophilization of the particles occurs and the contact angle drops to values lower than 90° and the emulsions becomes o/w again [249]. Similar effects have been reported using particles chemically modified to present different degrees of hydrophobicity [250]. The effect of the changes of particle wettability can be also used for foam stabilization [251–253]. However, no studies of the transition from aqueous foams to structures formed by free aqueous drops surrounded by a particle shell using surfactant to tune the hydrophilicity of the particles are present in the literature. However, these latter structures, dry water or liquid marbles, have been obtained using hydrophobic particles [254, 255].

It is also important to consider the role of the menisci formed by the contact line. Different studies have pointed out that the non-uniform wetting of the particles can affect the energetic landscape and the ability of particles to stabilize dispersed systems [80, 97, 196]. Ally *et al.* [256] demonstrate that the adhesion of particles to fluid interfaces depends on the particle wettability and edge geometry, which is important for controlling the behavior of particle-laden interface. Furthermore, the role of the menisci deformation due to gravitational effects for particles bigger enough cannot be neglected as a potential source of destabilization [257].

The effectiveness of colloidal particles in stabilising emulsions and foams depends in part on the formation of a sufficiently dense layer of particles at the interface. The rheological properties of the interfacial layers also change as the concentration of particles at the interface increases and complete surface coverage is achieved. For high particle concentration the interfaces exhibit viscoelastic behaviour. The viscous properties govern rheological properties at low concentrations, while the elastic properties are dominant at high particle concentrations. The elastic contribution to the viscoelastic behaviour is largely due to the inter-particle interaction between particles. These interactions become significant at sufficiently high particle concentration. The viscoelastic nature of the interfaces affects the stability by decreasing the rate of film thinning between coalescing droplets.

It was mentioned above that the mechanical behaviour of interfaces, both shear and dilational, plays an essential role for controlling the interfacial stability and the deformation properties of coated drops and bubbles. It can be expected that the destabilization by drainage can be partially prevented by the increase of the shear viscosity and the dilational modulus [194]. Several authors have tried to deepen on the correlations existing between the interfacial properties of particle-laden interfaces and the stabilization of dispersed systems [53, 66, 242, 258, 259]. Cervantes-Martínez *et al.* [258] proposed that particle-laden interfaces presenting high resistance to the compression allows one to increase the stability of foams due to the decrease of the shrinking of small bubbles. They used the Gibbs criterion to establish the conditions for the stabilization of dispersed systems on the basis of the relationship between the surface tension and the dilational elasticity. According to the Gibbs criterion, only those particle-laden interfaces verifying that $E > \gamma/2$, with E being the elastic modulus,

can be stable. Stocco *et al.* [53] extended the application of the Gibbs criterion to the description of the stabilization of emulsions. However, their results pointed out that such approach is only valid when emulsions or foams are formed by spherical drops or bubbles. Furthermore, the studies by Stocco *et al.* [53] showed that gel-like interfaces present the better capacities to stability dispersed systems in agreement with the above discussed effect of the interfacial jamming. However, recent works have contributed to the controversy about the correlations existing between the rheological properties and the stabilization of dispersed systems. Santini *et al.* [79, 110, 112, 260] showed that the use of carbon particles allows one to stabilize foams and emulsion, even though they do not found any correlation between the stability of the dispersed systems and their rheological properties. This controversy is also feed by the studies of the stabilization of foam and emulsions by mixtures of silica nanoparticles and palmitic acid [111, 258]. Silica nanoparticles decorated with palmitic acid do not allow foam stabilization, even though the dilational viscoelastic modulus present relative high values (> 100 mN/m) [53]. However, the stabilization of emulsions at the water/hexane interface was possible with a poor dependence of the emulsion stability on the rheological properties [111].

The above discussion concerns so far to the role of the dilational modulus on the stabilization of dispersed systems. However, the influence of the shear modulus is clearly due to its close correlation to the interfacial structure and coverage. Several authors have shown that the formation of gel-like layers is essential for a good stabilization of the dispersed systems [190, 200, 261]. This was confirmed by Brugger *et al.* [262] using poly(N-isopropylacrylamide) particles for the stabilization of emulsions, pointing out that high values of G' provides good conditions for the emulsion stabilization, whereas the opposite is true for high values of G'' .

The ability of particle-laden interface to provide a high stability of foams and emulsions has provided the bases for their use as template for the production of porous materials, *e.g.* solid foams. These materials can be obtained by drying and sintering the wet system or directly by the solidification of the bulk liquid phase [15, 16]. Gonzenbach *et al.* [253, 263] take advantage of this idea for the stabilization of solid foams using liquid foams stabilized by mixtures of particles and different short length surfactant as precursors. Zabiegał *et al.* used similar approaches to prepare particle stabilized solid foams with carbonaceous and alumina particles [110, 264, 265].

10 Conclusions

The interest for understanding the physico-chemical bases governing the formation and properties of particle-laden interfaces has undergone a significant growth in recent years due to their implication in several technological and industrial fields. Despite the noticeable experimental and theoretical efforts to unravel the complex physics underlying the behavior of these systems a comprehensive descrip-

tion is difficult. This is in part due to the many parameters affecting its behavior: particle size, chemical nature, morphology, nature of the interface. On the other side, this allows controlling the morphology and mechanical properties of the formed layers. This has a big importance in the preparation of complex and hierarchical systems bases on particle-laden interfaces. Many experimental efforts have focused their interest on the understanding the equilibrium and dynamics properties of adsorbed and spread layers of particles at fluid interfaces. However, there exists a lack of theoretical work to correlate the experimental finding with accurate models. Thus, the fully understanding of the behavior of particle-laden interface requires multidisciplinary efforts. This review has tried to present critically the state of art of the topic, showing the level of understanding achieved in recent years in the description of the behavior of such intriguing systems.

This work was funded by MINECO under grant CTQ-2016-78895-R and carried out in the framework of the COST Action MP-1305. Authors thank R.G. Rubio, F. Ortega, L. Liggieri and F. Ravera for their support along these years.

Author contribution statement

The three authors has contributed equally in the preparation and discussion of the present review.

References

1. V. Lotito, T. Zambelli, *Adv. Colloid Interface Sci.* **246**, 217 (2017).
2. V. Garbin, *Phys. Today* **66**, 68 (2015) issue No. 10.
3. V. Garbin, J.C. Crocker, K.J. Stebe, *J. Colloid Interface Sci.* **387**, 1 (2012).
4. A. Maestro, E. Guzmán, F. Ortega, R.G. Rubio, *Curr. Opin. Colloid Interface Sci.* **19**, 355 (2014).
5. A. Maestro, E. Santini, D. Zabiegał, S. Llamas, F. Ravera, L. Liggieri, F. Ortega, R.G. Rubio, E. Guzman, *Adv. Condens. Matter Phys.* **2015**, 917516 (2015).
6. A.J. Mendoza, E. Guzmán, F. Martínez-Pedrero, H. Ritacco, R.G. Rubio, F. Ortega, V.M. Starov, R. Miller, *Adv. Colloid Interface Sci.* **206**, 303 (2014).
7. J.H.J. Thijssen, J. Vermant, *J. Phys.: Condens. Matter* **30**, 023002 (2018).
8. A. Maestro, E. Guzmán, E. Santini, in *Rheology: Principles, Applications and Environmental Impacts*, edited by E. Karpushkin (Nova Publishing, New York, USA, 2015) p. 1.
9. L.J. Bonales, F. Martínez-Pedrero, M.A. Rubio, R.G. Rubio, F. Ortega, *Langmuir* **28**, 16555 (2012).
10. L.J. Bonales, J.E.F. Rubio, H. Ritacco, C. Vega, R.G. Rubio, F. Ortega, *Langmuir* **27**, 3391 (2011).
11. E. Guzmán, E. Santini, L. Liggieri, F. Ravera, G. Loglio, A. Maestro, R.G. Rubio, J. Krägel, D. Grigoriev, R. Miller, in *Colloid and Interface Chemistry for Nanotechnology*, edited by P. Kralchevsky, R. Miller, F. Ravera (CRC Press, Taylor & Francis, Boca Raton, FL, USA, 2013) p. 77.

12. *Colloidal Particles at Liquid Interfaces*, edited by B.P. Binks, T.S. Horozov (Cambridge University Press, Cambridge, UK, 2006).
13. B.P. Binks, Phys. Chem. Chem. Phys. **9**, 6298 (2007).
14. B.P. Binks, Langmuir **33**, 6947 (2017).
15. A.R. Studart, U.T. Gonzenbach, E. Tervoort, L.J. Gauckler, J. Am. Ceram. Soc. **89**, 1771 (2006).
16. A.R. Studart, U.T. Gonzenbach, I. Akartuna, E. Tervoort, L.J. Gauckler, J. Mater. Chem. **17**, 3283 (2007).
17. E. Guzmán, S. Llamas, A. Maestro, L. Fernández-Peña, A. Akanno, R. Miller, F. Ortega, R.G. Rubio, Adv. Colloid Interface Sci. **233**, 38 (2016).
18. S. Llamas, E. Guzmán, F. Ortega, N. Baghdadli, C. Cazeneuve, R.G. Rubio, G.S. Luengo, Adv. Colloid Interface Sci. **222**, 461 (2015).
19. A.D. Dinsmore, M.F. Hsu, M.G. Nikolaidis, M. Marquez, A.R. Bausch, D.A. Weitz, Science **298**, 1006 (2002).
20. O.D. Velev, A.M. Lenhoff, E.W. Kaler, Science **287**, 2240 (2000).
21. O.D. Velev, S. Gupta, Adv. Mat. **21**, 1987 (2009).
22. E. Dickinson, Curr. Opin. Colloid Interface Sci. **15**, 40 (2010).
23. J. Ralston, D. Fornasiero, R. Hayes, Int. J. Miner. Process. **56**, 133 (1999).
24. E. Guzmán, A. Mateos-Maroto, M. Ruano, F. Ortega, R.G. Rubio, Adv. Colloid Interface Sci. **249**, 290 (2017).
25. E. Guzmán, L. Liggieri, E. Santini, M. Ferrari, F. Ravera, J. Phys. Chem. C **115**, 21715 (2011).
26. E. Guzmán, M. Ferrari, E. Santini, L. Liggieri, F. Ravera, Colloids Surf. B **136**, 971 (2015).
27. A. Moskal, T.R. Sosnowski, L. Gradon, in *Nanoparticles in Medicine and Environment*, edited by J.C.M. Marijnissen, L. Gradon (Springer Science+Business Media, Berlin-Heidelberg, 2011) p. 113.
28. K. Kramak-Romanowska, M. Odziomek, T.R. Sosnowski, Colloids Surf. A **480**, 149 (2015).
29. T.R. Sosnowski, Curr. Opin. Colloid Interface Sci. **36**, 1 (2018).
30. P.H.M. Hoet, I. Brüske-Hohlfeld, O.V. Salata, J. Nanobiotechnol. **2**, 12 (2004).
31. L. Bragg, J.F. Nye, Proc. R. Soc. London Ser. A: Math. Phys. Eng. Sci. **190**, 474 (1974).
32. A.J. Hurd, D.W. Schaefer, Phys. Rev. Lett. **54**, 1043 (1985).
33. W.L. Cheng, S.J. Dong, E.K. Wang, J. Phys. Chem. B **109**, 11548 (2005).
34. P. Pieranski, Phys. Rev. Lett. **45**, 569 (1980).
35. V. Garbin, J.C. Crocker, K.J. Stebe, Langmuir **28**, 1663 (2012).
36. D. Orsi, L. Cristofolini, G. Baldi, A. Madsen, Phys. Rev. Lett. **108**, 105701 (2012).
37. D. Orsi, A. Vezzani, R. Burioni, A. Pucci, G. Ruggeri, L. Cristofolini, Colloids Surf. A **441**, 912 (2014).
38. G.G. Fuller, J. Vermant, Annu. Rev. Chem. Biomol. Eng. **3**, 519 (2012).
39. R.G. Larsson, *The Structure and Rheology of Complex Fluids* (Oxford University Press, Oxford, UK, 1999).
40. R. Miller, L. Liggieri (Editors), *Interfacial Rheology* (Brill, Leiden, The Netherlands, 2010).
41. L. Liggieri, R. Miller, Curr. Opin. Colloid Interface Sci. **15**, 256 (2010).
42. W. Ramsden, Proc. R. Soc. London **72**, 156 (1903).
43. S.U. Pickering, J. Chem. Soc. Faraday Trans. **91**, 2001 (1907).
44. C. Zeng, H. Bissig, A.D. Dinsmore, Solid State Commun. **139**, 547 (2006).
45. D.Y. Zang, E. Rio, D. Langevin, B. Wei, B.P. Binks, Eur. Phys. J. E **31**, 125 (2010).
46. E. Santini, J. Krägel, F. Ravera, L. Liggieri, R. Miller, Colloids Surf. A **382**, 186 (2011).
47. A. Maestro, E. Guzman, E. Santini, F. Ravera, L. Liggieri, F. Ortega, R.G. Rubio, Soft Matter **8**, 837 (2012).
48. B.P. Binks, Curr. Opin. Colloid Interface Sci. **7**, 21 (2002).
49. F. Ravera, M. Ferrari, L. Liggieri, R. Miller, A. Passerone, Langmuir **13**, 4817 (1997).
50. F. Bresme, M. Oettel, J. Phys.: Condens. Matter **19**, 413101 (2007).
51. M. Oettel, S. Dietrich, Langmuir **24**, 1425 (2008).
52. D.Y. Zang, E. Rio, G. Delon, D. Langevin, B. Wei, B.P. Binks, Mol. Phys. **109**, 1057 (2011).
53. A. Stocco, E. Rio, B.P. Binks, D. Langevin, Soft Matter **7**, 1260 (2011).
54. L.D. Landau, *Fluid Mechanics* (Pergamon Press, London, UK, 1959).
55. A.W. Neumann, R. David, Y. Zuo, *Applied Surface Thermodynamics* (CRC Press, Taylor & Francis, Boca Raton, FL, USA, 1996).
56. D.Y. Zang, A. Stocco, D. Langevin, B.B. Wei, B.P. Binks, Phys. Chem. Chem. Phys. **11**, 9522 (2009).
57. A. Stocco, G. Su, M. Nobili, M. In, D. Wang, Soft Matter **10**, 6999 (2014).
58. V.N. Paunov, Langmuir **19**, 7970 (2003).
59. L.N. Arnaudov, O.J. Cayre, M.A. Cohen-Stuart, S.D. Stoyanov, V.N. Paunov, Phys. Chem. Chem. Phys. **12**, 328 (2010).
60. E.L. Sharp, H. Al-Shehri, T.S. Horozov, S.D. Stoyanov, V.N. Paunov, RSC Adv. **4**, 2205 (2014).
61. T.S. Horozov, D.A. Braz, P.D.I. Fletcher, B.P. Binks, J.H. Clint, Langmuir **24**, 1678 (2008).
62. T.N. Hunter, G.J. Jameson, E.J. Wanless, Aust. J. Chem. **60**, 651 (2007).
63. T.N. Hunter, J.G. Jameson, E.J. Wanless, D. Dupin, S.P. Armes, Langmuir **25**, 3440 (2009).
64. D.O. Grigoriev, J. Kragel, V. Dutschk, R. Miller, H. Mohwald, Phys. Chem. Chem. Phys. **9**, 6447 (2007).
65. D.O. Grigoriev, H. Mohwald, D.G. Shchukin, Phys. Chem. Chem. Phys. **10**, 1975 (2008).
66. A. Stocco, W. Drenckhan, E. Rio, D. Langevin, B.P. Binks, Soft Matter **5**, 2215 (2009).
67. L. Isa, F. Lucas, R. Wepf, E. Reimhult, Nat. Commun. **2**, 438 (2011).
68. I.B. Ivanov, P.A. Kralchevsky, A.D. Nikolov, J. Colloid Interface Sci. **112**, 97 (1986).
69. M. Zeng, J. Mi, C. Zhong, Phys. Chem. Chem. Phys. **13**, 3932 (2011).
70. A. Stocco, M. Nobili, Adv. Colloid Interface Sci. **247**, 223 (2017).
71. S.P. McBride, B.M. Law, Phys. Rev. Lett. **109**, 196101 (2012).
72. S. Levine, B.D. Bowen, S.J. Partridge, Colloids Surf. **38**, 325 (1989).
73. H.S. Wi, S. Cingarapu, K.J. Klabunde, B.M. Law, Langmuir **27**, 9979 (2011).

74. D.M. Kaz, R. McGorty, M. Mani, M.P. Brenner, V.N. Manoharan, *Nat. Mater.* **11**, 138 (2012).
75. P.D.I. Fletcher, B.L. Holt, *Langmuir* **27**, 12869 (2011).
76. C. Petcu, V. Purcar, C.-I. Spataru, E. Alexandrescu, R. Somoghi, B. Trica, S.G. Nitu, D.M. Panaitescu, D. Donescu, M.-L. Jecu, *Nanomaterials* **7**, 47 (2017).
77. E. Guzmán, H. Ritacco, F. Ortega, T. Svitova, C.J. Radke, R.G. Rubio, *J. Phys. Chem. B* **113**, 7128 (2009).
78. F. Ravera, E. Santini, G. Loglio, M. Ferrari, L. Liggieri, *J. Phys. Chem. B* **110**, 19543 (2006).
79. E. Santini, F. Ravera, M. Ferrari, M. Alfè, A. Ciajolo, L. Liggieri, *Colloids Surf. A* **365**, 189 (2010).
80. A. Maestro, L.J. Bonales, H. Ritacco, R.G. Rubio, F. Ortega, *Phys. Chem. Chem. Phys.* **12**, 14115 (2010).
81. L.C. Bradley, W.-H. Chen, K.J. Steebe, D. Lee, *Adv. Colloid Interface Sci.* **30**, 25 (2017).
82. M.A. Fernandez-Rodriguez, Y. Song, M.A. Rodríguez-Valverde, S. Chen, M.A. Cabrerizo-Vilchez, R. Hidalgo-Alvarez, *Langmuir* **30**, 1799 (2014).
83. M.A. Fernandez-Rodriguez, J. Ramos, L. Isa, M.A. Rodriguez-Valverde, M.A. Cabrerizo-Vilchez, R. Hidalgo-Alvarez, *Langmuir* **31**, 8818 (2015).
84. M.A. Fernandez-Rodriguez, L. Chen, C.P. Deming, M.A. Rodriguez-Valverde, S. Chen, M.A. Cabrerizo-Vilchez, R. Hidalgo-Alvarez, *Soft Matter* **12**, 31 (2016).
85. M.P. Boneva, N.C. Christov, K.D. Danov, P.A. Kralchevsky, *Phys. Chem. Chem. Phys.* **9**, 6371 (2007).
86. B.J. Park, J.P. Pantina, E.M. Furst, M. Oettel, S. Reynaert, J. Vermant, *Langmuir* **24**, 1686 (2008).
87. D.F. Williams, J.C. Berg, *J. Colloid Interface Sci.* **152**, 218 (1992).
88. C.S. Dias, P.J. Yunker, A.G. Yodh, N.A.M. Araújo, M.M.T.d. Gama, *Soft Matter* **14**, 1903 (2018).
89. P.J. Yunker, M.A. Lohr, T. Still, A. Borodin, D.J. Durian, A.G. Yodh, *Phys. Rev. Lett.* **110**, 035501 (2013).
90. C.S. Dias, N.A.M. Araújo, M.M.T.d. Gama, *EPL* **107**, 56002 (2014).
91. K. Masschaele, B.J. Park, E.M. Furst, J. Fransaer, J. Vermant, *Phys. Rev. Lett.* **105**, 048303 (2010).
92. F.H. Stillinger, *J. Chem. Phys.* **35**, 1584 (1961).
93. A.J. Hurd, *J. Phys. A: Math. Gen.* **18**, L1055 (1985).
94. D. Frydel, S. Dietrich, M. Oettel, *Phys. Rev. Lett.* **99**, 118302 (2007).
95. W. Bigui, C. Qing, Y. Caiyun, *J. Colloid Interface Sci.* **276**, 307 (2012).
96. J.P. Hansen, I.R. McDonald, *Theory of Simple Liquids* (Academic Press, London, UK, 2006).
97. D. Stamou, C. Duschl, D. Johannsmann, *Phys. Rev. E* **62**, 5263 (2000).
98. K.D. Danov, P.A. Kralchevsky, M.P. Boneva, *Langmuir* **20**, 6139 (2004).
99. O.S. Deshmukh, D. van den Ende, M.C. Stuart, F. Mugele, M.H.G. Duits, *Adv. Colloid Interface Sci.* **222**, 215 (2015).
100. A.W. Adamson, A.P. Gast (Editors), *Physical Chemistry of Surfaces* (John Wiley & Sons, Inc., MA, USA, 1997).
101. R. Miller, V.B. Fainerman, V.I. Kovalchuk, D.O. Grigoriev, M.E. Leser, M. Michel, *Adv. Colloid Interface Sci.* **128-130**, 17 (2006).
102. V.B. Fainerman, V.I. Kovalchuk, E.H. Lucassen-Reynders, D.O. Grigoriev, J.K. Ferri, M.E. Leser, M. Michel, R. Miller, H. Mohwald, *Langmuir* **22**, 1701 (2006).
103. V.B. Fainerman, R. Miller, *Langmuir* **15**, 1812 (1999).
104. R.D. Groot, S.D. Stoyanov, *Soft Matter* **6**, 1682 (2010).
105. A. Mulero (Editor), *Theory and Simulation of Hard-Sphere Fluids and Related Systems* (Springer, Berlin, Germany, 2008).
106. A. Mulero, I. Cachadia, J.R. Solana, *Mol. Phys.* **107**, 1457 (2009).
107. O.S. Deshmukh, A. Maestro, M.H.G. Duits, D. van den Ende, M.A. Cohen-Stuart, F. Mugele, *Soft Matter* **28**, 7045 (2014).
108. F. Ravera, M. Ferrari, L. Liggieri, G. Loglio, E. Santini, A. Zanobini, *Colloids Surf. A* **323**, 99 (2008).
109. L. Liggieri, E. Santini, E. Guzmán, A. Maestro, F. Ravera, *Soft Matter* **7**, 6699 (2011).
110. D. Zabiegaj, E. Santini, E. Guzmán, M. Ferrari, L. Liggieri, V. Buscaglia, M.T. Buscaglia, G. Battilana, F. Ravera, *Colloids Surf. A* **438**, 132 (2013).
111. E. Santini, E. Guzmán, M. Ferrari, L. Liggieri, *Colloids Surf. A* **460**, 333 (2014).
112. D. Zabiegaj, E. Santini, E. Guzmán, M. Ferrari, L. Liggieri, F. Ravera, *J. Nanosci. Nanotechnol.* **15**, 3618 (2015).
113. E. Santini, E. Guzmán, F. Ravera, M. Ferrari, L. Liggieri, *Phys. Chem. Chem. Phys.* **14**, 607 (2012).
114. A.G. Bykov, G. Loglio, R. Miller, B.A. Noskov, *Colloids Surf. A* **485**, 42 (2015).
115. A.G. Bykov, B.A. Noskov, G. Loglio, V.V. Lyadinskaya, R. Miller, *Soft Matter* **10**, 6499 (2014).
116. P.A. Yazhgur, B.A. Noskov, L. Liggieri, S.-Y. Lin, G. Loglio, R. Miller, F. Ravera, *Soft Matter* **9**, 3305 (2013).
117. B.A. Noskov, P.A. Yazhgur, L. Liggieri, S.Y. Lin, G. Loglio, R. Miller, F. Ravera, *Colloid J.* **76**, 127 (2014).
118. B.A. Noskov, A.G. Bykov, *Curr. Opin. Colloid Interface Sci.* **37**, 1 (2018).
119. L. Parolini, A.D. Law, A. Maestro, D.M.A. Buzza, P. Cicuta, *J. Phys.: Condens. Matter* **27**, 194119 (2015).
120. F. Martinez-Pedrero, J. Benet, J.E.F. Rubio, E. Sanz, R.G. Rubio, F. Ortega, *Phys. Rev. E* **89**, 7 (2014).
121. A.B.D. Brown, C.G. Smith, A.R. Rennie, *Phys. Rev. E* **62**, 951 (2000).
122. N. Bowden, F. Arias, T. Deng, G.M. Whitesides, *Langmuir* **17**, 1757 (2001).
123. J.C. Loudet, A.G. Yodh, B. Pouligny, *Phys. Rev. Lett.* **97**, 018304 (2006).
124. F. Kim, S. Kwan, J. Akana, P. Yang, *J. Am. Chem. Soc.* **123**, 4360 (2001).
125. J.L. Hernández-López, E.R. Alvizo-Páez, S.E. Moya, J. Ruiz-García, *J. Phys. Chem. B* **110**, 23179 (2006).
126. J.C. Loudet, A.M. Alsayed, J. Zhang, A.G. Yodh, *Phys. Rev. Lett.* **94**, 018301 (2005).
127. H. Lehle, E. Noruzifar, M. Oettel, *Eur. Phys. J. E* **26**, 151 (2008).
128. L. Botto, L. Yao, R.L. Leheny, K.J. Stebe, *Soft Matter* **8**, 4971 (2012).
129. L. Isa, N. Samudrala, E.R. Dufresne, *Langmuir* **30**, 5057 (2014).
130. C.S. Dias, N.A.M. Araújo, M.M. Telo da Gama, *Adv. Colloid Interface Sci.* **247**, 258 (2017).
131. C.S. Dias, N.A.M. Araújo, M.M. Telo da Gama, *Phys. Rev. E* **90**, 032302 (2014).
132. N.A.M. Araújo, C.S. Dias, M.M.T.d. Gama, *J. Phys.: Condens. Matter* **27**, 194123 (2015).
133. D. Frenkel, *Physica A* **313**, 1 (2002).

134. J.K.G. Dhont, *An Introduction to Dynamics of Colloids* (Elsevier, Amsterdam, The Netherlands, 1996).
135. E. Guzmán, J. Tajuelo, J.M. Pastor, M.Á. Rubio, F. Ortega, Ramón G. Rubio, *Curr. Opin. Colloid Interface Sci.* **37**, 33 (2018).
136. A. Maestro, D. Jones, C.S.d.R. Candela, E. Guzman, M.H.G. Duits, P. Cicuta, *Langmuir* **34**, 7067 (2018).
137. J. Tajuelo, E. Guzmán, F. Ortega, R.G. Rubio, M.A. Rubio, *Langmuir* **33**, 4280 (2017).
138. J. Tajuelo, P.J.M., M.A. Rubio, *J. Rheol.* **60**, 1095 (2016).
139. L. Cristofolini, D. Orsi, L. Isa, *Curr. Opin. Colloid Interface Sci.* **37**, 13 (2018).
140. G. Boniello, C. Blanc, D. Fedorenko, M. Medfai, N.B. Mbarek, M. In, M. Gross, A. Stocco, M. Nobili, *Nat. Mater.* **14**, 908 (2015).
141. L.J. Bonales, PhD Thesis, Universidad Complutense de Madrid, 2009.
142. Y. Peng, W. Chen, T.M. Fischer, D.A. Weitz, P. Tong, *J. Fluid Mech.* **618**, 243 (2009).
143. S. Mazoyer, F. Ebert, G. Maret, P. Keim, *EPL* **88**, 66004 (2009).
144. S. Mazoyer, F. Ebert, G. Maret, P. Keim, *Eur. Phys. J. E* **34**, 101 (2011).
145. L. Cipelletti, H. Bissig, V. Trappe, P. Ballesta, S. Mazoyer, *J. Phys.: Condens. Matter* **15**, S257 (2003).
146. D.C. Morse, in *Advances in Chemical Physics*, edited by S.A. Rice (John Wiley & Sons, Hoboken, USA, 2004).
147. P.N. Pusey, W. van Meegen, *Physica A* **157**, 705 (1989).
148. M. Bellour, M. Skouri, J.-P. Munch, P. Hébraud, *Eur. Phys. J. E* **8**, 431 (2002).
149. J. Galvan-Miyoshi, J. Delgado, R. Castillo, *Eur. Phys. J. E* **26**, 369 (2008).
150. P. Keim, G. Maret, U. Herz, H.H. von Grünberg, *Phys. Rev. Lett.* **21**, 215504 (2004).
151. Y.N. Ohshima, I. Nishio, *J. Chem. Phys.* **114**, 8649 (2001).
152. R. Miller, J.K. Ferri, A. Javadi, J. Krägel, N. Mucic, R. Wüstneck, *Colloid Polym. Sci.* **288**, 937 (2010).
153. F. Monroy, F. Ortega, R.G. Rubio, M.G. Velarde, *Adv. Colloid Interfaces Sci.* **134-135**, 175 (2007).
154. F. Ortega, H. Ritacco, R.G. Rubio, *Curr. Opin. Colloid Interface Sci.* **15**, 237 (2010).
155. H. Hilles, F. Monroy, L.J. Bonales, F. Ortega, R.G. Rubio, *Adv. Colloid Interface Sci.* **122**, 67 (2006).
156. C.P. Whitby, E.J. Wanless, *Materials* **9**, 626 (2016).
157. B.A. Noskov, *Adv. Colloid Interface Sci.* **69**, 63 (1996).
158. A. Maestro, E. Guzmán, R. Chuliá, F. Ortega, R.G. Rubio, R. Miller, *Phys. Chem. Chem. Phys.* **13**, 9534 (2011).
159. C. Kotsmar, V. Pradines, V.S. Alahverdijeva, E.V. Akse- nenko, V.B. Fainerman, V.I. Kovalchuk, J. Krägel, M.E. Leser, B.A. Noskov, R. Miller, *Adv. Colloid Interface Sci.* **150**, 41 (2009).
160. A. Akanno, E. Guzmán, L. Fernández-Peña, S. Llamas, F. Ortega, R.G. Rubio, *Langmuir* **34**, 7455 (2018).
161. M. Safouane, D. Langevin, B.P. Binks, *Langmuir* **23**, 11546 (2007).
162. K. Zahn, A. Wille, G. Maret, S. Sengupta, P. Nielaba, *Phys. Rev. Lett.* **90**, 155506 (2003).
163. D.Y. Zang, Y.J. Zhang, Q.W. Hou, *Colloids Surf. A* **395**, 262 (2012).
164. T. Kobayashi, M. Kawaguchi, *J. Colloid Interface Sci.* **390**, 147 (2013).
165. O.I. del Río, D.Y. Kwok, R. Wu, J.M. Alvarez, A.W. Neumann, *Colloids Surf. A* **143**, 197 (1998).
166. C.D. Bain, P.M. Claesson, D. Langevin, R. Meszaros, T. Nylander, C. Stubenrauch, S. Titmuss, R. von Klitzing, *Adv. Colloid Interface Sci.* **155**, 32 (2010).
167. I. Varga, R.A. Campbell, *Langmuir* **33**, 5915 (2017).
168. S. Llamas, L. Fernandez-Pena, A. Akanno, E. Guzman, V. Ortega, F. Ortega, A.G. Csaky, R.A. Campbell, R.G. Rubio, *Phys. Chem. Chem. Phys.* **20**, 1395 (2018).
169. S. Llamas, E. Guzmán, A. Akanno, L. Fernández-Peña, F. Ortega, R.A. Campbell, R. Miller, R.G. Rubio, *J. Phys. Chem. C* **122**, 4419 (2018).
170. H. Wang, W. Lu, B. Chen, *Appl. Surf. Sci.* **254**, 3380 (2008).
171. C.P. Whitby, D. Fornasiero, J. Ralston, L. Liggieri, F. Ravera, *J. Phys. Chem. C* **116**, 3050 (2012).
172. E. Guzman, L. Liggieri, E. Santini, M. Ferrari, F. Ravera, *Colloids Surf. A* **413**, 280 (2012).
173. E. Guzman, L. Liggieri, E. Santini, M. Ferrari, F. Ravera, *Soft Matter* **8**, 3938 (2012).
174. E. Guzman, L. Liggieri, E. Santini, M. Ferrari, F. Ravera, *Colloids Surf. B* **105**, 284 (2013).
175. D. Orsi, E. Guzmán, L. Liggieri, F. Ravera, B. Ruta, Y. Chushkin, T. Rimoldi, L. Cristofolini, *Sci. Rep.* **5**, 17930 (2015).
176. E. Guzman, E. Santini, D. Zabiegaj, M. Ferrari, L. Liggieri, F. Ravera, *J. Phys. Chem. C* **119**, 26937 (2015).
177. E. Guzman, E. Santini, M. Ferrari, L. Liggieri, F. Ravera, *J. Phys. Chem. C* **119**, 21024 (2015).
178. D. Orsi, T. Rimoldi, E. Guzman, L. Liggieri, F. Ravera, B. Ruta, L. Cristofolini, *Langmuir* **32**, 4868 (2016).
179. E. Guzman, E. Santini, M. Ferrari, L. Liggieri, F. Ravera, *Langmuir* **33**, 10715 (2017).
180. E. Guzman, D. Orsi, L. Cristofolini, L. Liggieri, F. Ravera, *Langmuir* **30**, 11504 (2014).
181. D. Langevin, *Light Scattering by Liquid Surfaces and Complementary Techniques* (Marcel Dekker, New York, USA, 1992).
182. J.D. Ferry, *Viscoelastic Properties of Polymers* (Wiley, New York, USA, 1980).
183. J.J. Gray, R.T. Bonnecaze, *J. Rheol.* **42**, 1121 (1998).
184. P. Cicuta, E.J. Stancik, G.G. Fuller, *Phys. Rev. Lett.* **90**, 236101 (2003).
185. V. Trappe, D.A. Weitz, *Phys. Rev. Lett.* **85**, 449 (2000).
186. S. Reynaert, P. Moldenaers, J. Vermant, *Phys. Chem. Chem. Phys.* **9**, 6463 (2007).
187. C.M. Wijmans, E. Dickinson, *Langmuir* **14**, 7278 (1998).
188. L. Imperiali, K.-H. Liao, C. Clasen, J. Fransaer, C.W. Macosko, J. Vermant, *Langmuir* **28**, 7990 (2012).
189. S. Barman, G.F. Christopher, *Langmuir* **30**, 9752 (2014).
190. B. Madivala, J. Fransaer, J. Vermant, *Langmuir* **25**, 2718 (2009).
191. M.G. Basavaraj, G.G. Fuller, J. Fransaer, J. Vermant, *Langmuir* **22**, 6605 (2006).
192. E. Brown, H. Zhang, N.A. Forman, B.W. Maynor, D.E. Betts, J.M. DeSimone, H.M. Jaeger, *Phys. Rev. E* **84**, 031408 (2011).
193. E.J. Stancik, M.J.O. Widenbrant, A.T. Laschitsch, J. Vermant, G.G. Fuller, *Langmuir* **18**, 4372 (2002).
194. Z. Cui, *Phys. Rev. E* **83**, 031911 (2011).
195. H.J. Wilson, R.H. Davis, *J. Fluid Mech.* **452**, 425 (2002).
196. A. San-Miguel, S.H. Behrens, *Langmuir* **28**, 12038 (2012).

197. M. Zanini, C. Marschelke, S.E. Anachkov, E. Marini, A. Synytska, L. Isa, *Nat. Commun.* **8**, 15701 (2017).
198. D. Zang, D. Langevin, B.P. Binks, B. Wei, *Phys. Rev. E* **81**, 011604 (2010).
199. H.-L. Cheng, S.S. Velankar, *Langmuir* **25**, 4412 (2009).
200. S. Vandebriel, J. Vermant, P. Moldenaers, *Soft Matter* **6**, 3353 (2010).
201. R. Krishnaswamy, S. Majumdar, R. Ganapathy, V.V. Agarwal, A.K. Sood, C.N.R. Rao, *Langmuir* **23**, 3084 (2007).
202. D. Orsi, G. Baldi, P. Cicutta, L. Cristofolini, *Colloids Surf. A* **413**, 71 (2012).
203. D. Orsi, B. Ruta, Y. Chushkin, A. Pucci, G. Ruggeri, G. Baldi, T. Rimoldi, L. Cristofolini, *Phys. Rev. E* **89**, 042308 (2014).
204. A.A. Saberi, *Phys. Rep.* **578**, 1 (2015).
205. J.W. Essam, *Rep. Prog. Phys.* **43**, 833 (1980).
206. M. Maas, C.C. Ooi, G.G. Fuller, *Langmuir* **26**, 17867 (2010).
207. P. Degen, M. Paulus, M. Maas, R. Kahner, S. Schmacke, B. Struth, M. Tolan, H. Rehage, *Langmuir* **24**, 12958 (2008).
208. P. Degen, D.C.F. Wieland, S. Leick, M. Paulus, H. Rehage, M. Tolan, *Soft Matter* **7**, 7655 (2011).
209. S.J. Ebbens, *Curr. Opin. Colloid Interface Sci.* **21**, 14 (2016).
210. Y.S. Ryazantsev, M.G. Velarde, R.G. Rubio, E. Guzmán, F. Ortega, P. López, *Adv. Colloid Interface Sci.* **247**, 52 (2017).
211. F. Martinez-Pedrero, P. Tierno, *Phys. Rev. Appl.* **3**, 051003 (2015).
212. F. Martinez-Pedrero, A. Cebers, P. Tierno, *Soft Matter* **12**, 3688 (2016).
213. F. Martinez-Pedrero, H. Massana-Cid, T. Ziegler, T.H. Johansen, A.V. Straube, P. Tierno, *Phys. Chem. Chem. Phys.* **18**, 26353 (2016).
214. F. Martinez-Pedrero, A. Cebers, P. Tierno, *Phys. Rev. Appl.* **6**, 034002 (2016).
215. F. Martinez-Pedrero, A. Cebers, P. Tierno, *Soft Matter* **12**, 3688 (2016).
216. H. Massana-Cid, F. Martinez-Pedrero, E. Navarro-Argemi, I. Pagonabarraga, P. Tierno, *New J. Phys.* **19**, 103031 (2017).
217. H. Massana-Cid, F. Martinez-Pedrero, A. Cebers, P. Tierno, *Phys. Rev. E* **96**, 012607 (2017).
218. F. Martinez-Pedrero, H. Massana-Cid, P. Tierno, *Small* **13**, 1603449 (2017).
219. F. Martinez-Pedrero, E. Navarro-Argemi, A. Ortiz-Ambriz, I. Pagonabarraga, P. Tierno, *Sci. Adv.* **4**, 9379 (2018).
220. W. Fei, Y. Gu, K.J.M. Bishop, *Curr. Opin. Colloid Interface Sci.* **32**, 57 (2017).
221. F. Martinez-Pedrero, A. Ortiz-Ambriz, I. Pagonabarraga, P. Tierno, *Phys. Rev. Lett.* **115**, 138301 (2015).
222. B.A. Grzybowski, H.A. Stone, G.M. Whitesides, *Nature* **405**, 1033 (2000).
223. N. Mano, A. Heller, *J. Am. Chem. Soc.* **127**, 11574 (2005).
224. Y. Wang, R.M. Hernandez, D.J. Bartlett, J.M. Bingham, T.R. Kline, A. Sen, T.E. Mallouk, *Langmuir* **22**, 10451 (2006).
225. J.L. Moran, P.M. Wheat, J.D. Posner, *Phys. Rev. E* **81**, 065302 (2010).
226. M. Driscoll, B. Delmotte, M. Youssef, S. Sacanna, A. Donev, *Nat. Phys.* **13**, 375 (2017).
227. P. Magaretti, M.N. Popescu, S. Dietrich, M. Tasinkevych, *Soft Matter* **12**, 4007 (2016).
228. X. Wang, M. In, C. Blanc, M. Nobili, A. Stocco, *Soft Matter* **11**, 7376 (2015).
229. J. Koplik, C. Maldarelli, *Phys. Rev. Fluids* **2**, 024303 (2017).
230. X. Wang, M. In, C. Blanc, P. Magaretti, M. Nobili, A. Stocco, *Faraday Discuss.* **191**, 305 (2016).
231. J. Yuan, S.K. Cho, *J. Mech. Sci. Technol.* **26**, 3761 (2012).
232. V. Pimienta, C. Antoine, *J. Colloid Interface Sci.* **19**, 290 (2014).
233. L.E. Scriven, C.V. Sternling, *Nature* **187**, 186 (1960).
234. B.P. Binks (Editor), *Modern Aspects of Emulsion Science* (The Royal Society of Chemistry, Cambridge, UK, 1998).
235. A. Lucia, A.C. Toloza, E. Guzmán, F. Ortega, R.G. Rubio, *PeerJ* **5**, e3171 (2017).
236. A. Lucia, P.G. Argudo, E. Guzmán, R.G. Rubio, F. Ortega, *Colloids Surf. A* **521**, 133 (2017).
237. S. Llamas, E. Santini, L. Liggieri, F. Salerni, D. Orsi, L. Cristofolini, F. Ravera, *Langmuir* **34**, 5978 (2018).
238. R. Aveyard, B.P. Binks, J.H. Clint, *Adv. Colloid Interface Sci.* **100**, 503 (2003).
239. N.J. Alvarez, S.L. Anna, T. Saigal, R.D. Tilton, L.M. Walker, *Langmuir* **28**, 8052 (2012).
240. T.S. Horozov, R. Aveyard, J.H. Clint, B. Neumann, *Langmuir* **21**, 2330 (2005).
241. K. Stratford, R. Adhikari, I. Pagonabarraga, J.C. Desplat, M.E. Cates, *Science* **309**, 2198 (2005).
242. A. Maestro, E. Rio, W. Drenckhan, D. Langevin, A. Salonen, *Soft Matter* **10**, 6975 (2014).
243. W.J. Frith, R. Pichot, M. Kirkland, B. Wolf, *Ind. Eng. Chem. Res.* **47**, 6434 (2008).
244. A.P. Sullivan, P.K. Kilpatrick, *Ind. Eng. Chem. Res.* **41**, 3389 (2002).
245. V.B. Menon, D.T. Wasan, *Sep. Sci. Technol.* **23**, 2131 (1988).
246. E.J. Stancik, G.G. Fuller, *Langmuir* **20**, 4805 (2004).
247. D. Tambe, M.M. Sharma, *Adv. Colloid Interface Sci.* **52**, 1 (1994).
248. B.P. Binks, L. Isa, A.T. Tyowua, *Langmuir* **29**, 4923 (2013).
249. B.P. Binks, J.A. Rodrigues, *Angew. Chem. Int. Ed.* **46**, 5389 (2007).
250. T. Kostakis, R. Ettelaie, S.B. Morray, *Langmuir* **22**, 1273 (2006).
251. B.P. Binks, M. Kirkland, J.A. Rodrigues, *Soft Matter* **4**, 2373 (2008).
252. U.T. Gonzenbach, A.R. Studart, E. Tervoort, L.J. Gauckler, *Langmuir* **22**, 10983 (2006).
253. U.T. Gonzenbach, A.R. Studart, E. Tervoort, L.J. Gauckler, *Angew. Chem. Int. Ed.* **118**, 3606 (2006).
254. A. Bajwa, Y. Xu, A. Hashmi, M. Leong, L. Ho, J. Xu, *Soft Matter* **8**, 11604 (2012).
255. B.P. Binks, R. Murakami, *Nat. Mater.* **5**, 865 (2006).
256. J. Ally, M. Kappl, H.-J. Butt, *Langmuir* **28**, 11042 (2012).
257. P.A. Kralchevsky, K. Nagayama, *Adv. Colloid Interface Sci.* **85**, 145 (2000).
258. A. Cervantes-Martinez, E. Rio, G. Delon, A. Saint-Jalmes, D. Langevin, B.P. Binks, *Soft Matter* **4**, 1531 (2008).

259. L.R. Arriaga, W. Drenckhan, A. Salonen, J.A. Rodrigues, RamonIniguez-Palomares, E. Rio, D. Langevin, *Soft Matter* **8**, 11085 (2012).
260. E. Santini, E. Guzmán, F. Ravera, A. Ciajolo, M. Alfè, L. Liggieri, M. Ferrari, *Colloids Surf. A* **413**, 216 (2012).
261. J.K. Kim, P.A. Rühls, P. Fischer, J.S. Hong, *Rheol. Acta* **52**, 327 (2013).
262. B. Brugger, J. Vermant, W. Richtering, *Phys. Chem. Chem. Phys.* **12**, 14573 (2010).
263. U.T. Gonzenbach, A.R. Studart, E. Tervoort, L.J. Gauckler, *Langmuir* **23**, 1025 (2007).
264. D. Zabiegaj, E. Santini, M. Ferrari, L. Liggieri, F. Ravera, *Colloids Surf. A* **473**, 24 (2015).
265. D. Zabiegaj, M.T. Buscaglia, D. Giuranno, L. Liggieri, F. Ravera, *Microporous Mesoporous Mater.* **239**, 45 (2017).